

fsemipar: an R package for SoF semiparametric regression

Silvia Novo* Germán Aneiros**

*Statistics Department, Universidad Carlos III de Madrid

**Mathematics Department, CITIC, Universidade da Coruña

Abstract

Functional data analysis has become a tool of interest in applied areas such as economics, medicine, and chemistry. Among the techniques developed in recent literature, functional semiparametric regression stands out for its balance between flexible modelling and output interpretation. Despite the large variety of research papers dealing with scalar-on-function (SoF) semiparametric models, there is a notable gap in software tools for their implementation. This article introduces the R package `fsemipar`, tailored for these models. `fsemipar` not only estimates functional single-index models using kernel smoothing techniques but also estimates and selects relevant scalar variables in semi-functional models with multivariate linear components. A standout feature is its ability to identify impact points of a curve on the response, even in models with multiple functional covariates, and to integrate both continuous and pointwise effects of functional predictors within a single model. In addition, it allows the use of location-adaptive estimators based on the k -nearest-neighbours approach for all the semiparametric models included. Its flexible interface empowers users to customise a wide range of input parameters and includes the standard S3 methods for prediction, statistical analysis, and estimate visualization (`predict`, `summary`, `print`, and `plot`), enhancing clear result interpretation. Throughout the article, we illustrate the functionalities and the practicality of `fsemipar` using two chemometric datasets.

Keywords: R package; functional data analysis; semiparametric regression; functional single-index model; semi-functional models; variable selection; impact point selection; k -nearest neighbours

1 Introduction

The technological advances of recent decades have enabled the recording of vast amounts of data, leading to a revolution in data analysis. Applied disciplines now require tools to handle complex datasets, posing ongoing challenges for statisticians in both methodological and computational aspects. For example, real-world applications often involve an extensive number of random variables. Data may even be infinite-dimensional; that is, the observations of these variables are measured either continuously or in a finely-spaced grid over a time interval, over a surface or even more intricate structures. For instance, in economics, intraday stock price can be considered as a curve (see, e.g., [Rice et al. 2020](#)); in chemometrics, the measurement of a spectrometer results in a curve (see, e.g.,

Dai and Genton 2018); in medicine, magnetic resonance imaging outputs are images (see, e.g. Li et al. 2019). In such cases, data “atoms” are random functions, leading to the categorization of this data type as *functional data*.

The term *Functional Data Analysis* (FDA) encompasses those statistical methods designed to handle functional data. Currently, functional regression has garnered significant attention within the statistical community. In particular, scalar-on-function (SoF) regression, i.e. the case of scalar response and functional covariates, has emerged as a prolific area of research (see Greven and Scheipl 2017 and Reiss et al. 2017 for recent reviews). Several SoF regression models have been formulated, including parametric, nonparametric, and semiparametric approaches (if we follow the terminology of conventional finite-dimensional regression). Parametric models, like the functional linear model (see, e. g., chapter 12 of Ramsay and Silverman 2005 for a comprehensive description and Febrero-Bande et al. 2017 for a discussion on estimation techniques), provide a straightforward practical interpretation but are limited in terms of flexibility. In contrast, nonparametric models (see, e. g., Ferraty and Vieu 2006 for a detailed development and Ling and Vieu 2018 for a review) provide a high level of flexibility, but the outputs are challenging to interpret. As a middle point, semiparametric regression (see Ling and Vieu 2021 for a recent survey) provides a balance between parametric and nonparametric approaches allowing for flexible models while yielding interpretable results.

The practical application of functional linear and functional nonparametric regression has been facilitated by computational tools designed for their implementation, typically developed within the R programming environment (R Core Team 2022). Among these, the R packages `fda` (see Ramsay et al. 2022) and `fda.usc` (see Febrero-Bande and Oviedo de la Fuente 2012) stand out as key references in the FDA field. In the context of SoF regression, the former allows for the estimation of the functional linear model using the techniques described in Ramsay and Silverman 2005. The latter includes several parametric and nonparametric functional regression models. It can estimate the functional linear model using several approaches (including those described in Cardot et al. 1999, Ramsay and Silverman 2005 and Preda and Saporta 2005), the functional nonparametric model (described in Ferraty and Vieu 2006) and various generalised additive models for functional data (described in Febrero-Bande and González-Manteiga 2013). There are also two other major packages designed specifically for regression problems involving functional variables: `FDBoost` (see Brockhaus et al. 2020) and `refund` (see Goldsmith et al. 2023). In the SoF context, the package `FDBoost` fits additive models using a component-wise gradient boosting algorithm. It allows for functional and scalar covariates, but the effects of functional predictors currently implemented are functional linear and smooth interactions. Regarding the `refund` package, it implements penalised functional regression, including generalised additive models for functional data using spline-based methods (developed in McLean et al. 2014).

While there are other packages tailored to specific models and applications (see Scheipl et al. 2022 for an overview of R packages for functional data analysis), to the best of our knowledge there was no R package dealing with the estimation of functional single-index models prior to the introduction of `fsemipar`. It is worth noting that despite the practical advantages of functional semiparametric regression over parametric and nonparametric approaches, implementation is usually complex and requires advanced knowledge of mathematical programming. To address this gap, we created the R package `fsemipar` (see Aneiros and Novo 2024) aiming to simplify the use of SoF semiparametric models. It can estimate functional single-index models (see Amato et al. 2006) and can also simultaneously esti-

mate and select relevant scalar variables in models composed of a multivariate linear component and either a functional single-index part (see [Novo et al. 2021a](#)) or a functional nonparametric part (see [Aneiros et al. 2015](#)). For that, it allows both kernel-based and k -nearest-neighbours-based estimators, allowing the user to choose between a global smooth or a location-adaptive one. A remarkable feature of `fsemipar` is the selection of impact points of a curve on the scalar response variable (see [Aneiros and Vieu 2014](#)). Essentially, this means the package can incorporate discretised observations from a curve into the regression model. From these observations, it then identifies and selects the most predictive points of the discretisation interval, termed “impact points” or “points of impact”. As a consequence, it allows for the inclusion of both pointwise and continuous effects of functional variables in the response (see [Aneiros and Vieu 2015](#) and [Novo et al. 2021b](#)), leading to interpretability, model simplification and good predictive performance. An important feature of its functions is their ability to accommodate a wide range of customisable input parameters. This flexibility enables expert users to achieve a more precise fit. At the same time, the functions require only the data as a mandatory argument, thereby simplifying usage for non-experts.

In this tutorial, we present the R package `fsemipar`, available from the Comprehensive R Archive Network (CRAN) at <https://CRAN.R-project.org/package=fsemipar>. The remainder of the paper is structured as follows. Section 2 addresses SoF semiparametric regression with a single functional covariate. Section 3 deals with SoF semiparametric models incorporating multiple scalar predictors and a functional covariate. Section 4 discusses SoF semiparametric regression with multiple scalar predictors derived from the discretization of a curve and a functional covariate. The three sections share the same structure (I=2,3,4): Section I.1 introduces the modeling approaches implemented in `fsemipar`, Section I.2 summarizes the techniques for estimating such models, and Section I.3 presents the software infrastructure, introducing the main functions and classes of the package `fsemipar` tailored for each model. To highlight the capabilities of the package, Section I.3 also contains practical applications using two real datasets from the chemometric field. Finally, Section 5 includes a discussion about the functions included and some directions for future development. Due to space constraints, we have not delved into every facet of the package. For a detailed description of each function, readers are directed to the package manual.

2 Single functional covariate

In Section 2, we focus on SoF semiparametric models with single functional predictor. Section 2.1 introduces the functional single-index model as a competitor of the linear model and the nonparametric model. In Section 2.2, we discuss the estimation techniques implemented in `fsemipar`. Finally, Section 2.3 presents the associated functions of the package and illustrates their use with a real chemometric dataset.

2.1 The functional single-index model

Let Y be a scalar random variable, \mathcal{X} (also denoted as $\mathcal{X}(t)$ with $t \in \mathcal{I}$ and $\mathcal{I} \subset \mathbb{R}$) a functional covariate valued in some infinite-dimensional space \mathcal{H} , and ε , a random error. We assume that we observe data pairs $\{(Y_i, \mathcal{X}_i), i = 1, \dots, n\}$ independent and identically distributed (i.i.d.) to (Y, \mathcal{X}) .

We are interested in predict Y using \mathcal{X} .

Literature in FDA focused on three different regression strategies to address this situation:

- *The linear (parametric) approach.* The functional linear model (FLM) is formulated under the assumption of a linear relationship between the functional covariate and the response, represented as: $Y_i = \int_{\mathcal{I}} \theta_0(t) \mathcal{X}_i(t) dt + \varepsilon_i$ $i = 1, \dots, n$. Here, $\mathcal{H} = L^2(\mathcal{I})$ and θ_0 is an unknown parameter-function defined on \mathcal{I} . One of the strengths of this model is its ability to provide an interpretable output, θ_0 , and its relative ease of estimation compared to alternative models. The main disadvantage is that it may not be reliable in some real applications due to its dependence on the linearity assumption.
- *The nonparametric approach.* To address the inflexibility of the FLM, a natural step is to move away from the strict linear hypothesis and instead adopt a basic smooth condition. This lead us to the functional nonparametric model (FNM) given by the expression: $Y_i = m(\mathcal{X}_i) + \varepsilon_i$ $i = 1, \dots, n$. In this context, \mathcal{H} is a semimetric space and $m(\cdot)$ an unknown, smooth, non-linear functional operator. The FNM is more reliable than the FLM in practice, but $m(\cdot)$ is harder to represent and interpret, and also more difficult to estimate.
- *The semiparametric approach.* To combine the strengths of both parametric and nonparametric approaches, an appealing technique is to assume that the functional predictor acts on the response only through its projection onto some one-dimensional subspace. This leads to the functional single-index model (FSIM), represented as:

$$Y_i = r(\langle \theta_0, \mathcal{X}_i \rangle) + \varepsilon_i, \quad i = 1, \dots, n. \quad (1)$$

In this case, \mathcal{H} is a separable Hilbert space and $\langle \cdot, \cdot \rangle$ denotes its the inner product; $\theta_0 \in \mathcal{H}$ is the functional index: a function-parameter that allows to summarize the information carried in \mathcal{X}_i to predict Y_i , and r is the unknown, non-linear, smooth link function. The FSIM can be viewed as an extension of the FLM, offering enhanced flexibility due to the smooth link function r . Conversely, it can be considered a specific instance of the FNM, but with the advantage of dimensionality reduction, given that r operates on a scalar rather than a function like $m(\cdot)$. As a consequence, the FSIM offers interpretable and representable outputs (θ_0 and r).

We can implement the FLM using several R functions: `fRegress` (estimation based on basis representation) of the `fda` R package, as well as the functions `fregre.basis` (estimation based on basis representation), `fregre.pc` (functional principal component estimation) and `fregre.pls` (partial least-squares estimation) of the `fda.usc` package. For the implementation of the FNM, we can use the function `fregre.np` (nonparametric kernel estimation) of the `fda.usc` package. We can also refer to the codes created by F. Ferraty, available on his website: <https://www.math.univ-toulouse.fr/~ferraty/SOFTWARES/NPFDA/index.html>. However, to the best of our knowledge, there is no function available for the direct implementation of the FSIM. In the subsequent section, we will introduce the techniques for estimating the FSIM that are included in the `fsemipar` package.

2.2 Link function and functional index estimation

Since the FSIM can be seen as a particular case of the FNM, we can estimate the former by adapting the estimation techniques used for the latter. In this section, we will briefly discuss how this is achieved. It is important to note that the package can also estimate models with functional nonparametric components. This capability is precisely why we have explored functional nonparametric estimation in depth throughout this section.

Ferraty and Vieu (2006) proposed the functional extension of the classical Nadaraya-Watson kernel estimator (see Nadaraya, 1964 and Watson, 1964) for the FNM. The following expression provides the kernel estimator for $m(\cdot)$:

$$\widehat{m}_h(\chi) = \frac{\sum_{i=1}^n Y_i K(h^{-1}d(\mathcal{X}_i, \chi))}{\sum_{i=1}^n K(h^{-1}d(\mathcal{X}_i, \chi))}, \quad \forall \chi \in \mathcal{H}. \quad (2)$$

Here, $h \in \mathbb{R}^+$ represents the bandwidth, d is a general semi-metric, which allows the computation of the proximity between functional data, and K is a real-valued asymmetrical kernel.

Alternatively, Burba et al. (2009) studied the functional version of the k NN estimator (see Collomb, 1979 and Devroye et al., 1994, among others) for $m(\cdot)$. For each element χ within \mathcal{H} , it calculates the regression solely based on the k sample observations that exhibit the closest proximity to said element. Specifically, the k NN estimator for $m(\cdot)$ is defined as follows

$$\widehat{m}_k^*(\chi) = \frac{\sum_{i=1}^n Y_i K(H_{k,\chi}^{-1}d(\mathcal{X}_i, \chi))}{\sum_{i=1}^n K(H_{k,\chi}^{-1}d(\mathcal{X}_i, \chi))}, \quad \forall \chi \in \mathcal{H}. \quad (3)$$

Here, $k \in \mathbb{Z}^+$ is the tuning parameter and $H_{k,\chi} = \min\{h \in \mathbb{R}^+ \text{ such that } \sum_{i=1}^n 1_{B(\chi, h)}(\mathcal{X}_i) = k\}$, where $B(\chi, h) = \{z \in \mathcal{H} : d(\chi, z) \leq h\}$, the derived local bandwidth which depends on k . Unlike the kernel case, in the k NN estimator (3) the smoothing parameter $H_{k,\chi}$ depends on χ (and k), which provides the desired location-adaptive property. Furthermore, this local smoothing estimator exclusively relies on a discrete parameter k that takes values from a finite set $\{1, \dots, n\}$. This attribute presents an additional advantage over the kernel estimator, where selecting the tuning parameter h needs consideration of a continuous interval.

Regarding the tuning parameters, in FDA the typical approach for addressing the selection of h and k is cross-validation (CV), specifically, leave-one-out CV (LOOCV), where the objective functions are defined as

$$CV(h) = n^{-1} \sum_{j=1}^n \left(Y_j - \widehat{m}_h^{(-j)}(\mathcal{X}_j) \right)^2 \quad \text{and} \quad CV^*(k) = n^{-1} \sum_{j=1}^n \left(Y_j - \widehat{m}_k^{*(-j)}(\mathcal{X}_j) \right)^2,$$

respectively. Here, $\widehat{m}_h^{(-j)}(\cdot)$ and $\widehat{m}_k^{*(-j)}(\cdot)$ are the leave-one-out versions of $\widehat{m}_h(\cdot)$ and $\widehat{m}_k^*(\cdot)$, respectively. Then, we select $\widehat{h} = \arg \min_{h \in [a, b]} CV(h)$ and $\widehat{k} = \arg \min_{k \in \{k_1, \dots, k_2\}} CV^*(k)$. The theoretical validation of both the data-driven selectors was showed in Kara-Zaitri et al. (2017b,a). In practise, it is usual to minimize over an interval $[a, b] \subset \mathbb{R}^+$ (respectively, over a set $\{k_1, \dots, k_2\} \subset \{1, \dots, n\}$) that encompasses a range of reasonable values for h (k , respectively). The issue of automatically selecting the interval $[a, b]$ remains unresolved in one-dimensional nonparametric statistics. However, it is often considered of lesser importance due to the tendency of the CV function to exhibit relative flatness

around its minimum, see [Novo et al. \(2019\)](#). In Section 2.3.1 we delve into the options included in the `fsemipar` package.

In the functional context, we must pay attention to the selection of the semi-metric d : since \mathcal{H} represents an infinite-dimensional space, the equivalence between norms fails (in contrast to what happens in the finite-dimensional Euclidean space). [Ferraty and Vieu \(2006\)](#) provided some alternatives of semi-metric, like the based on the functional principal component expansion, on the Fourier expansion, and on the B-spline expansion of the derivatives. We can compute these semi-metrics through the functions `semimetric.pca`, `semimetric.fourier`, and `semimetric.deriv`, respectively, included in the `fd.usc` package.

An interesting special case arises when the semi-metric is contingent upon a parameter. This circumstance is observed in the FSIM (1), where we consider the operator $r_{\theta_0}(\cdot) : \mathcal{H} \rightarrow \mathbb{R}$ defined as $r_{\theta_0}(\chi) = r(\langle \theta_0, \chi \rangle)$, $\forall \chi \in \mathcal{H}$. In this special case, if we want to quantify the proximity between elements of the functional space to obtain a nonparametric estimator for $r_{\theta_0}(\cdot)$, the semi-metric adopts the following form:

$$d_{\theta_0}(\chi_1, \chi_2) = |\langle \theta_0, \chi_1 \rangle - \langle \theta_0, \chi_2 \rangle| = |\langle \theta_0, \chi_1 - \chi_2 \rangle|, \quad \text{for } \chi_1, \chi_2 \in \mathcal{H}, \quad (4)$$

thus relying on the function-parameter θ_0 . When θ_0 is unknown, the expressions (2) and (3) become statistics (and not estimators) since they also depend on a parameter and can't be directly employed in practice. That is, for each $\theta \in \mathcal{H}$, they turn into

$$\widehat{r}_{h,\theta}(\chi) = \frac{\sum_{i=1}^n Y_i K(h^{-1}d_{\theta}(\mathcal{X}_i, \chi))}{\sum_{i=1}^n K(h^{-1}d_{\theta}(\mathcal{X}_i, \chi))}, \quad \widehat{r}_{k,\theta}^*(\chi) = \frac{\sum_{i=1}^n Y_i K(H_{k,\chi,\theta}^{-1}d_{\theta}(\mathcal{X}_i, \chi))}{\sum_{i=1}^n K(H_{k,\chi,\theta}^{-1}d_{\theta}(\mathcal{X}_i, \chi))}, \quad \forall \chi \in \mathcal{H}. \quad (5)$$

Here, $H_{k,\chi,\theta} = \min \{h \in \mathbb{R}^+ \text{ such that } \sum_{i=1}^n 1_{B_{\theta}(\chi,h)}(\mathcal{X}_i) = k\}$ with $B_{\theta}(\chi,h) = \{z \in \mathcal{H} : d_{\theta}(\chi,z) \leq h\}$. In this scenario, the semi-metric selection is direct; however, as a trade-off, we are required to estimate θ_0 . To address the estimation of the regression in the FSIM (selection of tuning parameter and estimation of θ_0), we can use LOOCV. That is, considering the following objective functions

$$CV(h, \theta) = n^{-1} \sum_{j=1}^n \left(Y_j - \widehat{r}_{h,\theta}^{(-j)}(\mathcal{X}_j) \right)^2 \quad \text{and} \quad CV^*(k, \theta) = n^{-1} \sum_{j=1}^n \left(Y_j - \widehat{r}_{k,\theta}^{*(-j)}(\mathcal{X}_j) \right)^2, \quad (6)$$

respectively, and minimising them respect to both parameters. Consequently, the kernel-based and k NN-based estimators of θ_0 are

$$\widehat{\theta}_h = \arg \min_{\theta \in \Theta} CV(h, \theta), \quad \widehat{\theta}_k^* = \arg \min_{\theta \in \Theta} CV^*(k, \theta), \quad (7)$$

where $\Theta \subset \mathcal{H}$, while the selectors of h and k are, respectively, $\widehat{h} = \arg \min_{h \in [a,b]} CV(h, \widehat{\theta}_h)$, and $\widehat{k} = \arg \min_{k_1 \leq k \leq k_2} CV^*(k, \widehat{\theta}_k)$. By substituting these estimators into (5), we obtain $\widehat{r}_{\widehat{h}, \widehat{\theta}_h}(\chi)$ and $\widehat{r}_{\widehat{k}, \widehat{\theta}_k}^*(\chi)$, respectively. The theoretical validation of both the data-driven selectors for the tuning parameters (h or k) and the estimators for θ_0 was established by [Novo et al. \(2019\)](#).

The focal aspect in practical application is the implementation of the minimization problems described in equation (7) to estimate θ_0 . Note that the minimisation is performed on a subset of the functional space $\Theta \subset \mathcal{H}$, so the question of how to build this subset seems challenging. [Ait-Saïdi et al. \(2008\)](#)

or [Ferraty et al. \(2013\)](#) proposed to solve this issue using B-Spline approximation of the functional directions and reduce the infinite-dimensional optimization problem to a multivariate one. Specifically, each direction $\theta \in \Theta$ is obtained from a d -dimensional space generated by B-spline basis functions, denoted as $\{e_1(\cdot), \dots, e_d(\cdot)\}$. Consequently, our attention is focused on directions expressed as

$$\theta(\cdot) = \sum_{j=1}^d \alpha_j e_j(\cdot) \text{ where } (\alpha_1, \dots, \alpha_d) \in \mathcal{V}. \quad (8)$$

and the problem in expression (7) turns into:

$$\hat{\theta}_h = \arg \min_{(\alpha_1, \dots, \alpha_d) \in \mathcal{V}} CV(h, \theta), \quad \hat{\theta}_k^* = \arg \min_{(\alpha_1, \dots, \alpha_d) \in \mathcal{V}} CV^*(k, \theta). \quad (9)$$

To construct the set of coefficients \mathcal{V} in (8), it is necessary to consider the model identifiability conditions (see [Ferraty et al., 2003](#)). Such restrictions hold true when $\theta \in \Theta$ satisfies the constraints $\langle \theta, \theta \rangle = 1$ and $\theta(t_0) > 0$ for some arbitrary t_0 in the domain of θ_0 (see [Ait-Saïdi et al., 2008](#)).

Taking into account the outlined considerations, the `fsemipar` package includes two procedures to carry out the minimisation of the CV functions defined in (6): (i) a direct method based on [Ait-Saïdi et al. \(2008\)](#); (ii) an iterative algorithm based on [Ferraty et al. \(2013\)](#).

2.2.1 Procedure in [Ait-Saïdi et al. \(2008\)](#)

[Ait-Saïdi et al. \(2008\)](#) proposed the joint minimisation in the tuning parameter and the functional direction in (6). As a consequence, their method requires intensive computation. Thus, it is necessary to strike a balance between the size of Θ and the performance of the estimators. The following lines describe how to construct the set of coefficients \mathcal{V} in (8):

1. Choose the dimension of the B-spline basis d . We can decompose d as $d = \ell + n_r$, where ℓ is the order of the B-spline functions (degree $\ell - 1$) and n_r is the number of regularly spaced interior knots (see [De Boor 1978](#)).
2. For each $(\beta_1, \dots, \beta_d) \in \mathcal{C}^d$, where $\mathcal{C} = \{c_1, \dots, c_J\} \subset \mathbb{R}^J$ denotes a set of J “seed-coefficients”, build the initial functional direction

$$\theta_{init}(\cdot) = \sum_{j=1}^d \beta_j e_j(\cdot). \quad (10)$$

3. For each θ_{init} in Step 1 that verifies the condition $\theta_{init}(t_0) > 0$, where t_0 denotes a fixed value in the domain of $\theta_{init}(\cdot)$, compute $\langle \theta_{init}, \theta_{init} \rangle$ and construct

$$(\alpha_1, \dots, \alpha_d) = \frac{(\beta_1, \dots, \beta_d)}{\langle \theta_{init}, \theta_{init} \rangle^{1/2}}.$$

4. Construct \mathcal{V} as the set of vectors $(\alpha_1, \dots, \alpha_d)$ obtained in Step 2.

Therefore, the final set of eligible functional directions is given by

$$\Theta = \left\{ \theta(\cdot) = \sum_{j=1}^d \alpha_j e_j(\cdot); (\alpha_1, \dots, \alpha_d) \in \mathcal{V} \right\}.$$

Subsequently, the goal is to compute the value of the CV functions in (6) for each pair (θ, h) (respectively (θ, k)) where $\theta \in \Theta$, and select pair that minimises (6).

Remark 2.1. *To achieve a balance between computation time and accurate estimation, Ait-Saïdi et al. 2008 recommended using the seed-coefficients $\mathcal{C} = \{1, 0, -1\}$. This set has been shown to offer good practical performance (see Novo et al., 2019). Regarding the dimension of the B-spline basis, d , the usual procedure is to set the order of the B-spline functions (ℓ) and try different number of internal knots, n_r . Then, we can choose the value of n_r that minimises the CV function: $\hat{n}_r = \arg \min_{n_r \in \mathbb{Z}^+} CV(\hat{\theta}_{\hat{h}}, \hat{h})$ (respectively, $\hat{n}_r^* = \arg \min_{n_r \in \mathbb{Z}^+} CV^*(\hat{\theta}_{\hat{k}}, \hat{k})$).*

2.2.2 Procedure in Ferraty et al. (2013)

Instead of the direct joint minimisation, Ferraty et al. (2013) and Chan et al. (2023) proposed an iterative algorithm. For a given d :

1. Choose an initial set of coefficients $\boldsymbol{\gamma} = (\gamma_1, \dots, \gamma_d) \in \mathbb{R}^d$ to give rise to a functional direction $\theta^{(0,m)}$ as in (10). Calibrate them to verify the identifiability conditions of the model. As a result you obtain another set of coefficients $\boldsymbol{\alpha} = (\alpha_1, \dots, \alpha_d)$ corresponding to a functional direction $\theta^{(m)}$.
2. Select the optimal tuning parameter setting $\theta^{(m)}$ in (6): $\hat{h}^{(m)} = \arg \min_{h \in [a_m, b_m]} CV(h, \theta^{(m)})$ (respectively, $\hat{k}^{(m)} = \arg \min_{k_{m_1} < k < k_{m_2}} CV^*(k, \theta^{(m)})$).
3. Estimate the direction setting $\hat{h}^{(m)}$ (respectively, $\hat{k}^{(m)}$) in (6): $\hat{\theta}^{(0,m+1)} = \arg \min_{\boldsymbol{\gamma} \in \mathbb{R}^d} CV(\hat{h}^{(m)}, \boldsymbol{\gamma})$, $(\hat{\theta}^{*(0,m+1)} = \arg \min_{\boldsymbol{\gamma} \in \mathbb{R}^d} CV^*(\hat{k}^{(m)}, \boldsymbol{\gamma}))$.
4. Update $\theta^{(0,m)} = \hat{\theta}^{(0,m+1)}$ ($\theta^{(0,m)} = \hat{\theta}^{*(0,m+1)}$). Continue the process until convergence is achieved: the algorithm halts when the change in CV from one iteration to the next (scaled by the variance of the response) is positive and falls below a predetermined threshold.

Remark 2.2. *In step 3 of the method, the minimisation can be carried out using general-purpose optimisation algorithms for multidimensional spaces, such as Nelder and Mead (1965), included in the R function `optim`.*

2.3 Fitting the FSIM with the fsemipar package

The `fsemipar` package contains several functions for estimating the FSIM. It provides the flexibility to perform both kernel and k NN fitting, with implementation options based on either Ait-Saïdi et al. (2008) or Ferraty et al. (2013). The primary related functions are summarised in the Table 1. Each primary function produces an object that belongs to an S3 class. These S3 classes are designed to include essential S3 methods, such as `print()`, `summary()`, `plot()` and `predict()` to facilitate the posterior analysis. Each function offers a wide range of customisable parameters for the user, while also providing a straightforward option to use default settings for the input parameters.

Function	S3 class	Description
<code>fsim.kernel.fit</code>	'fsim.kernel'	kernel estimation based on Ait-Saïdi et al. (2008)
<code>fsim.kNN.fit</code>	'fsim.kNN'	k NN estimation based on Ait-Saïdi et al. (2008)
<code>fsim.kernel.fit.optim</code>	'fsim.kernel'	kernel estimation based on Ferraty et al. (2013)
<code>fsim.kNN.fit.optim</code>	'fsim.kNN'	k NN estimation based on Ferraty et al. (2013)

Table 1: Summary of main functions for the FSIM and associated S3 classes.

2.3.1 Main fitting functions

The main fitting functions for the FSIM (Table 1) implement either the procedure detailed in [Ait-Saïdi et al. \(2008\)](#) (`fsim.kernel.fit()` and `fsim.kNN.fit()`) or the procedure outlined in [Ferraty et al. \(2013\)](#) (`fsim.kernel.fit.optim()` and `fsim.kNN.fit.optim()`). In each case, these procedures are combined with either kernel or k NN estimation.

Regarding the functional predictor, all the functions of the package `fsemipar` require the values of the curves evaluated on a grid of equally-spaced discretisation points. The functions internally represent the discretised curves in a B-spline basis of dimension that can be customised by the user. Functions in Table 1 share two required arguments: the functional predictor \mathbf{x} , a matrix of dimension (n, p) containing n curves discretised in p points, and the scalar response variable \mathbf{y} , a vector of dimension n .

```
fsim.kernel.fit(x,y,...)
fsim.kNN.fit(x,y,...)
fsim.kernel.fit.optim(x,y,...)
fsim.kNN.fit.optim(x,y,...)
```

However, these functions also take several optional arguments for finer control:

- *Optional arguments for the nonparametric fit.* These arguments are summarised in Table 2 and refer to the type of kernel used and the choice of the tuning parameters: h (kernel), or k (k NN). In the kernel-based functions `fsim.kernel.fit()` and `fsim.kernel.fit.optim()`, there is a default option for constructing the sequence of bandwidths from which \hat{h} will be selected. This default option takes into account the proximity between sample curves using the semimetric (in the FSIM, the projection semimetric). Specifically, the endpoints of the sequence are determined by calculating quantiles of a certain order, controlled by the user through the arguments `min.q.h` (default 0.05) and `max.q.h` (default 0.5), of the distances between curves. Additionally, the number of bandwidths in the sequence can also be customised using `num.h` (default 10). Alternatively, we can directly specify the sequence of bandwidths with the argument `h.seq`. When `h.seq` is provided, the arguments `min.q.h`, `max.q.h` and `num.h` are ignored. Regarding k NN-based functions `fsim.kNN.fit()` and `fsim.kNN.fit.optim()`, the user has the flexibility to choose the endpoints of the sequence for k (number of neighbours) using `min.knn` (default 2) and `max.knn` (default integer division $n/5$). In addition, the user can specify the step between two consecutive elements of the sequence using the argument `step` (default smallest

integer greater than or equal to $n/100$). Alternatively, we can directly provide the sequence of number of neighbours using `knearest`. It is important to note that if we specify the `knearest` argument, `min.knn`, `max.knn` and `step` are ignored.

The four primary functions share the argument `kind.of.kernel` that allows user to choose the type of kernel function. Currently, only Epanechnikov kernel (“quad”) is available.

Function	Argument	Description
<code>fsim.kernel.fit</code> <code>fsim.kernel.fit.optim</code>	<code>min.q.h</code>	Minimum quantile order for the distances.
	<code>max.q.h</code>	Maximum quantile order for the distances.
	<code>num.h</code>	Number of h values in the sequence.
	<code>h.seq</code>	Sequence of h values.
<code>fsim.kNN.fit</code> <code>fsim.kNN.fit.optim</code>	<code>min.knn</code>	Minimum k for k NN fitting.
	<code>max.knn</code>	Maximum k for k NN fitting.
	<code>step</code>	Step between elements of the sequence.
	<code>knearest</code>	Sequence of k values.
All	<code>kind.of.kernel</code>	Type of kernel used.

Table 2: Optional input arguments related to nonparametric estimation (kernel or k NN).

- *Optional arguments for B-spline expansions.* These arguments are summarised in Table 3 and refer to the B-spline expansion for the functional directions and predictor. The four functions allow to customize the order of the B-spline functions, ℓ , through the argument `order.Bspline` (default 3), the number of interior knots, n_r , for directions in Θ using `nknot.theta` (default 3), and the number of interior knots for the sample curves with `nknot` (default $\text{floor}((p - \ell - 1)/2)$), and their definition interval with `range.grid`.

In addition, functions `fsim.kernel.fit()` and `fsim.kNN.fit()` allow to choose the set of seed coefficients \mathcal{C} through the argument `seed.coeff` (see Section 2.2.1). Furthermore, the functions `fsim.kernel.fit()` and `fsim.kNN.fit.optim()` enable the choice of the set of initial coefficients $\gamma \in \mathbb{R}^d$ through the argument `gamma`.

- *Optional arguments for the parallel computation.* For functions `fsim.kernel.fit()` and `fsim.kNN.fit()` the implementation is computationally expensive. For that, they both allow the parallel computation (internally, they use the functions `makeCluster()`, `registerDoParallel()`, and `foreach()` of the R packages `parallel`, `doParallel` and `foreach`, respectively). Users can explicitly specify the number of CPU cores to use for parallel execution with the argument `n.core`. By default, the both functions take `n.core` as the number of available cores minus 1 if more than 1 is available, otherwise 1 (this is done internally using the function `availableCores()` of the R package `parallel`). For sequential execution, it is sufficient to set `n.core=1`.
- *Optional arguments for controlling the iterative algorithm.* The functions `fsim.kernel.fit.optim()` and `fsim.kNN.fit.optim()` are built upon an iterative procedure (see Section 2.2.2).

Users have the flexibility to customize the convergence threshold using the argument `threshold` (default: 5e-3).

Function	Arguments	Description
<code>fsim.kernel.fit</code>	<code>order.Bspline</code>	Order of the B-spline basis functions.
<code>fsim.kNN.fit</code>	<code>nknot.theta</code>	Number of interior knots for the functional directions in Θ .
<code>fsim.kernel.fit.optim</code>	<code>nknot</code>	Number of interior knots for the curves.
<code>fsim.kNN.fit.optim</code>	<code>range.grid</code>	Endpoints of the definition interval for the curves.
<code>fsim.kernel.fit</code>	<code>seed.coeff</code>	Set of seed coefficients \mathcal{C} .
<code>fsim.kNN.fit</code>		
<code>fsim.kernel.fit.optim</code>	<code>gamma</code>	Set of initial coefficients γ .
<code>fsim.kNN.fit.optim</code>		

Table 3: Optional input arguments related to B-spline expansions.

2.3.2 Case study I, part I: Tecator dataset

The Tecator dataset is a well-known benchmark database in FDA, as evidenced by the numerous research works in the field that have used it to illustrate their techniques (see, e.g., [Amato et al. 2006](#), [Ferraty and Vieu 2006](#), [Galeano et al. 2015](#), among others). This dataset contains spectral measurements of 215 pork samples collected using a Tecator Infratec Food and Feed Analyser. The spectrum includes absorbances at 100 wavelengths in the range 850 to 1050 nm, which are commonly considered to be functional data. In addition, the dataset records the fat, protein and moisture content of each meat sample.

The Tecator dataset is included in the `fsemipar` package. In addition to the discretised original spectrometric curves, the first and second derivatives are included. Figure 1 includes a graphical representation of the first 20 curves (left panel) and its second derivative (right panel). We illustrate the primary FSIM fitting functions of the package by predicting the fat percentage using the available spectrometric data, specifically the second derivative of the curves (usual choice in the literature, see, e. g., [Aneiros and Vieu 2015](#), [Novo et al. 2019](#)). Note that spectrometric data is more readily obtainable, as analysing the chemical composition typically involves cost-intensive and lengthier chemical experiments. To evaluate the performance of the procedures we split the sample into two subsamples: the training sample is composed of the first 160 entries in the dataset, whereas the test sample includes the remaining 55 observations.

```
> data(Tecator)
> str(Tecator)
List of 6
 $ fat          : num [1:215] 22.5 40.1 8.4 5.9 25.5 42.7 42.7 10.6 19.9 19.9 ...
```

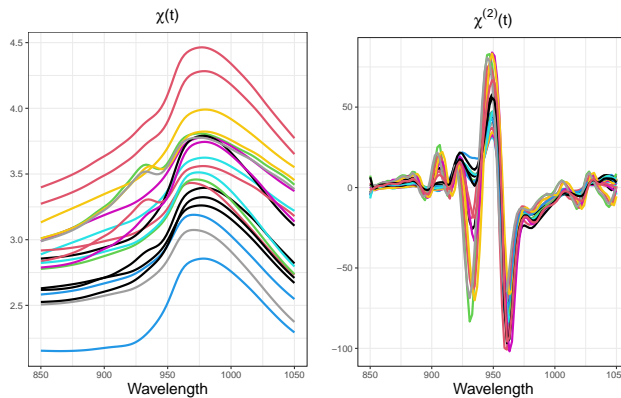


Figure 1: Sample of 20 spectrometric curves (left panel) and their second derivatives (right panel).

```

$ protein      : num [1:215] 16.7 13.5 20.5 20.7 15.5 13.7 13.7 19.3 17.7 17.7 ...
$ moisture    : num [1:215] 60.5 46 71 72.8 58.3 44 44 69.3 61.4 61.4 ...
$ absor.spectra : num [1:215, 1:100] 2.62 2.83 2.58 2.82 2.79 ...
$ absor.spectra1: num [1:215, 1:100] 0.0352 0.4171 0.1772 0.1776 0.168 ...
$ absor.spectra2: num [1:215, 1:100] 1.118 -4.412 -4.764 -6.778 -0.601 ...

```

As an example, the following code shows the implementation of the FSIM using the `fsim.kNN.fit()` function. In addition to the data, we have provided some specific input arguments to improve the fit: we have narrowed the sequence in which the number of neighbours is selected (setting `max.knn=15`), discarding the largest values which in this case lead to oversmoothing and an increment of the computational time. We also set `step=1` to try all the values in this sequence. Additionally, we have specified the number of interior knots for the B-spline representation of the unknown functional direction (`nknot.theta=4`) and for the curves (`nknot=20`), also providing the range in which the curves were observed (`range.grid=c(850,1050)`). It is important to note that it is reasonable to seek a very precise representation of the curves on the B-spline basis, which leads to the use of a B-spline basis of greater dimension than in the case of the functional directions. In fact, large values of `nknot.theta` will tend to undersmoothing and capture the noise of the training sample. Furthermore, the computational cost of estimating the functional direction is strongly related to `nknot.theta` (greater `nknot.theta` more intensive computation), as we can deduce from Figure 2. For these reasons, it is usually recommended to take `nknot.theta` between 2 and 8.

```

> y<-Tecator$fat
> x<-Tecator$absor.spectra2
> train=1:160
> test=161:215
> fit<-fsim.kNN.fit(y[train],x=x[train,],max.knn=15,nknot.theta=4,nknot=20,
  range.grid=c(850,1050),step=1)

```

The fitted object of the functions listed in the Table 1 contains useful information about the estimation performed: the fitted values for the response (`fitted.values`), the residuals (`residuals`),

the coefficients of $\hat{\theta}$ in the B-spline basis (`theta.est`), the selected value of the tuning parameter, \hat{h} (`h.opt`) or \hat{k} (`k.opt`), the coefficient of determination (`r.squared`), the residual variance (`var.res`), the degrees of freedom (`df`) or the minimum value of the CV function (`CV.opt`). The following code shows the information contained in the output of the function `fsim.knn.fit()`.

```
> names(fit)
[1] "fitted.values" "residuals"      "theta.est"      "k.opt"
[5] "r.squared"     "var.res"        "df"             "yhat.cv"
[9] "CV.opt"        "CV.values"      "H"              "m.opt"
[13] "theta.seq.norm" "k.seq"          "call"           "y"
[17] "x"             "n"              "kind.of.kernel" "range.grid"
[21] "nknot"         "order.Bspline" "nknot.theta"

> class(fit)
[1] "fsim.kNN"
```

Each fitted object belongs to an S3 class (see Table 1), which implements S3 methods. In the particular case of `fsim.knn.fit()` (class `fsim.kNN`), the returned object can be used in the functions `print.fsime.knn()` and `summary.fsime.knn()` to display summaries of the fitted model. It can also be employed in `predict.fsime.knn()` to obtain predictions for new curves (which can be provided using the `newdata` argument), and the mean squared error of prediction (MSEP) if the actual responses are provided via the `y.test` argument. The MSEP is calculated as follows:

$$\text{MSEP} = \frac{1}{n_{test}} \sum_{i=n+1}^{n+n_{test}} (Y_i - \hat{Y}_i)^2, \quad (11)$$

where n_{test} is the size of the test sample and \hat{Y}_i , the predicted values. The code below illustrates these functionalities:

```
> summary(fit)
*** FSIM fitted using knn estimation with Nadaraya-Watson weights ***

-Call: fsim.knn.fit(x = x[1:160, ], y = y[1:160], nknot.theta = 4,
max.knn = 15, step = 1, range.grid = c(850, 1050), nknot = 20)

-Number of neighbours (k): 9
-Theta coefficients in the B-spline basis: 0.1656316 -0.1656316 0
0.1656316 -0.1656316 0 0.1656316
-CV: 3.921117
-R squared: 0.9824381
-Residual variance: 3.323535 on 132.9207 degrees of freedom

> predict(fit,newdata=x[test,],y.test=y[test])$MSEP
[1] 2.68585
```

Regarding the prediction, Table 4 displays the MSEP corresponding to each primary fitting function when using the respective cross-validation (CV) selectors for n_r , h , or k and θ_0 . In this example, the k NN-based functions yield lower MSEP values than the kernel-based ones. Furthermore, the procedure described in Ait-Saïdi et al. (2008) results in a lower MSEP than the one presented in Ferraty et al. (2013). However, for the functions based on the former procedure, when we increase n_r (`nknot.theta`), the computation time also increases, while for the functions based on the latter, it remains constant. This fact can be observed in Figure 2, where we show the execution times for the four functions over n_r . Note that `fsim.kernel.fit()` and `fsim.kNN.fit()` use parallel computation and were executed with `n.core=19`. For each function we set all the remaining optional input parameters (in particular, `order.Bspline=3`) while we vary `nknot.theta`.

Function	\hat{n}_k	MSEP
<code>fsim.kernel.fit()</code>	4	3.49
<code>fsim.kNN.fit()</code>	4	2.69
<code>fsim.kernel.fit.optim()</code>	2	3.64
<code>fsim.kNN.fit.optim()</code>	4	2.81

Table 4: MSEP obtained for each function using the respective CV selectors for tuning parameters, functional index, and n_r .

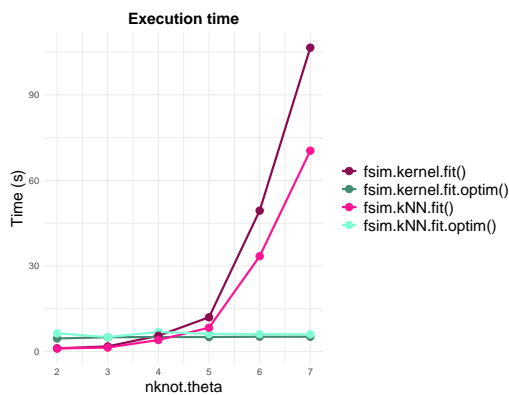


Figure 2: Execution time for functions in Table 1 over n_r obtained in a computer with the following features: Intel Core i9-10850K, 64GB, 1TB SSD and 2TB HDD, RTX 3090 24GB.

The S3 classes listed in Table 1 also implement the S3 method `plot()`. The routines implementing this S3 method use internally the R package `ggplot2`, trying to produce elegant and high quality charts. The output of this method represents the regression fit and the estimated functional index. In Figure 3, we provide the outputs of the 4 main functions when using the CV selectors for tuning parameters, functional index, and n_r .

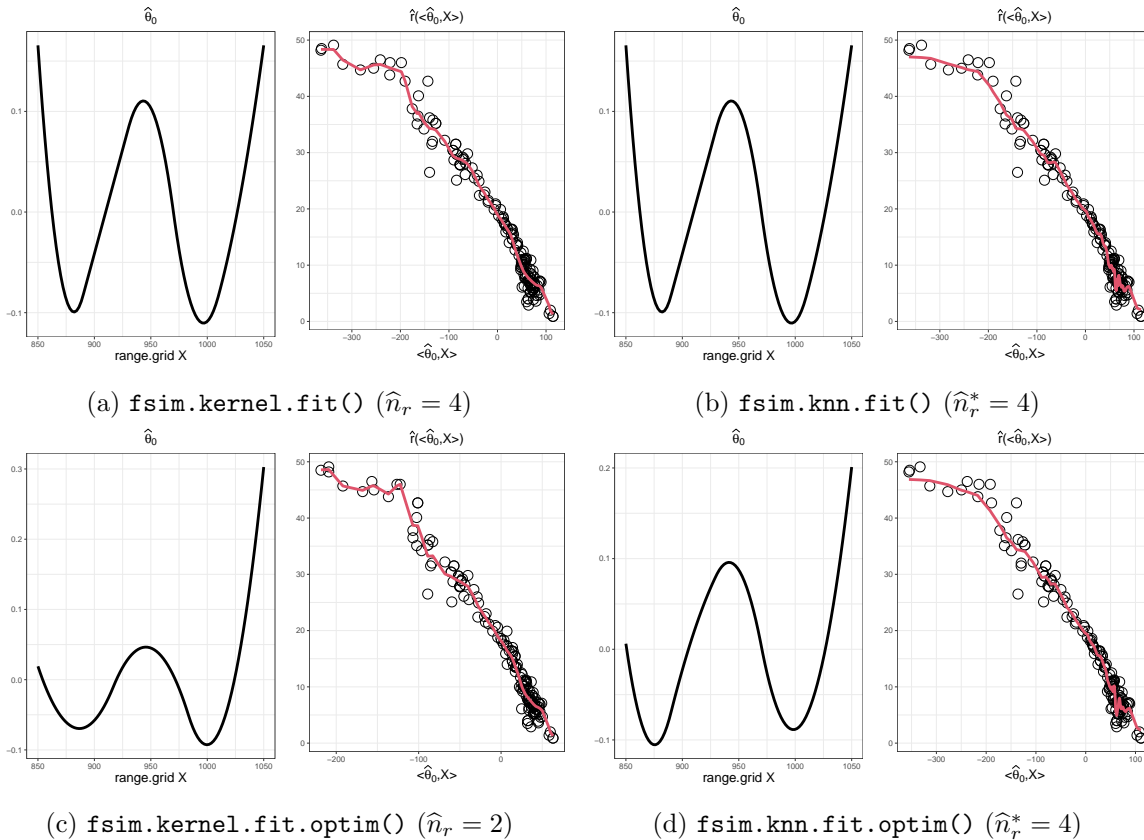


Figure 3: Outputs of the S3 method `plot()` applied to the fitted objects of functions in the Table 1, using the corresponding CV estimator for θ_0 and CV selectors for the tuning parameters and n_r .

3 Multiple scalar predictors and a functional covariate

In Section 3, we focus on SoF semiparametric regression including as predictors multiple scalar variables and a functional one. Section 3.1 introduces the modelling alternatives based on the partial linear structure. In Section 3.2, we discuss the techniques implemented in `fsemipar` for simultaneous estimation and variable selection in the linear component. Finally, Section 3.3 presents the associated functions of the package and illustrates their use with the Tecator dataset (see Section 2.3.2).

3.1 Semi-functional partial linear regression

In practical applications, it is common to encounter more than one covariate. Particularly, situations arise where, in addition to a functional predictor, several scalar variables are linked to the response. Take, for example, the Tecator dataset (see Section 2.3.2), which includes measurements of not only fat content but also the percentage of protein and moisture for each meat sample. These additional variables can be valuable in predicting fat content.

Statistically, this implies that, in addition to Y and \mathcal{X} , there exists a vector $\mathbf{Z} = (Z_1, \dots, Z_{p_n})^\top$ of scalar variables potentially related to the response. We observe tuples $\{(Y_i, \mathbf{Z}_i, \mathcal{X}_i), i = 1, \dots, n\}$ i.i.d. to $(Y, \mathbf{Z}, \mathcal{X})$ and our goal is to predict Y using the information carried by the remaining variables. In these complex scenarios, combining the partial linear approach with functional nonparametric or func-

tional single-index modelling typically yields interpretable results with good predictive performance. Consequently, literature in FDA focused on two regression strategies:

- The *semi-functional partial linear model* (SFPLM) (see [Aneiros-Pérez and Vieu 2006](#), [Aneiros et al. 2015](#), [Boente and Vahnovan 2017](#), among others), which is given by the expression

$$Y_i = Z_{i1}\beta_{01} + \cdots + Z_{ip_n}\beta_{0p_n} + m(\mathcal{X}_i) + \varepsilon_i \quad i = 1, \dots, n. \quad (12)$$

Here, $\beta_0 = (\beta_{01}, \dots, \beta_{0p_n})^\top$ is a vector of unknown real coefficients and $m(\cdot)$ is an unknown functional operator with the same features as in the FNM.

- The *semi-functional partial linear single-index model* (SFPLSIM) ([Wang et al. 2016](#), [Novo et al. 2021a](#)), which is given by the relationship

$$Y_i = Z_{i1}\beta_{01} + \cdots + Z_{ip_n}\beta_{0p_n} + r(\langle \theta_0, \mathcal{X}_i \rangle) + \varepsilon_i \quad i = 1, \dots, n. \quad (13)$$

Here, the vector $\beta_0 = (\beta_{01}, \dots, \beta_{0p_n})^\top \in \mathbb{R}^p$ is assumed to be unknown, as is the functional index $\theta_0 \in \mathcal{H}$ and the real-valued link function $r(\cdot)$, which both have the same characteristics as in the FSIM.

An interesting situation arises when only some of the p_n scalar covariates have a real effect on the response. Then estimation techniques must be combined with a variable selection tool.

The SFPLM, along with the kernel-based estimation procedure introduced in [Aneiros-Pérez and Vieu 2006](#), can be implemented in R using the function `fregre.plm` from the `fda.usc` package. However, it is worth noting that this function does not support variable selection in the linear component or k NN-based estimation. Furthermore, as far as we know, there is currently no function available for estimating the SFPLSIM and performing variable selection excluding those belonging to the `fsemipar` package. Consequently, in the subsequent section we introduce the techniques implemented in the `fsemipar` related to the SFPLM and SFPLSIM.

3.2 Estimation and variable selection in the linear component

[Aneiros et al. \(2015\)](#) introduced a procedure based on penalised least-squares (PeLS) for simultaneous estimation and variable selection in the linear component for the SFPLM (12). This procedure entails transforming the model into a linear model using nonparametric regression. Specifically:

1. The first step is to extract the effect of the functional covariate from the response and predictors:

$$Y_i - \mathbb{E}(Y_i|\mathcal{X}_i) = (\mathbf{Z}_i - \mathbb{E}(\mathbf{Z}_i|\mathcal{X}_i))^\top \beta_0 + \varepsilon_i, \quad i = 1, \dots, n, \quad (14)$$

where $\mathbf{Z}_i = (Z_{i1}, \dots, Z_{ip_n})$. Given that the expectations in the expression (14) are unknown, it becomes necessary to derive estimations for them. To accomplish this, we can employ functional nonparametric regression, utilizing either the kernel (2) or the k NN (3) estimators; so we need to choose an appropriate semimetric (see Section 2.2). After that, an approximate linear model is obtained:

$$\tilde{\mathbf{Y}} \approx \tilde{\mathbf{Z}}\beta_0 + \boldsymbol{\varepsilon}, \quad (15)$$

where $\tilde{\mathbf{Y}} = (\tilde{Y}_1, \dots, \tilde{Y}_n)^\top$ and $\tilde{\mathbf{Z}} = (\tilde{\mathbf{Z}}_1, \dots, \tilde{\mathbf{Z}}_n)^\top$ are the residuals of the regressions of the response variable and the predictors, respectively, over the functional covariate, and $\boldsymbol{\varepsilon} = (\varepsilon_1, \dots, \varepsilon_n)^\top$.

2. The second step entails the application of the PeLS approach to model (15), minimising the profile least-squares function with respect to $\boldsymbol{\beta} = (\beta_1, \dots, \beta_{p_n})^\top$:

$$\mathcal{Q}(\boldsymbol{\beta}) = \frac{1}{2} (\tilde{\mathbf{Y}} - \tilde{\mathbf{Z}}\boldsymbol{\beta})^\top (\tilde{\mathbf{Y}} - \tilde{\mathbf{Z}}\boldsymbol{\beta}) + n \sum_{j=1}^{p_n} \mathcal{P}_{\lambda_j}(\beta_j). \quad (16)$$

Here $\mathcal{P}_{\lambda_j}(\cdot)$ represents a penalty function and $\lambda_j > 0$ is a tuning parameter that controls the amount of penalisation. In fact, under suitable conditions on \mathcal{P}_λ (see, e.g., [Fan and Li 2001](#)), the PeLS estimators produce sparse solutions, that is, many estimated coefficients are zero (see [Aneiros et al. 2022](#) for a review on variable selection in the functional setting using shrinkage methods). Therefore, we perform simultaneous estimation and variable selection in the linear component.

3. The third step is the estimation of the functional operator $m(\cdot)$. After obtaining $\widehat{\boldsymbol{\beta}}_0$, a natural way to perform this estimation is to smooth the partial residuals, $Y_i - \mathbf{Z}_i^\top \widehat{\boldsymbol{\beta}}_0$. For that it is enough to replace Y_i by $Y_i - \mathbf{Z}_i^\top \widehat{\boldsymbol{\beta}}_0$ in (2) for kernel estimation, or in (3) for k NN techniques.

Regarding the choice of the penalty function $\mathcal{P}_\lambda(\cdot)$ in (16), there is a large list of possibilities in the literature for linear models. The LASSO ([Tibshirani 1996](#)), defined as $\mathcal{P}_\lambda(\beta_j) = \lambda |\beta_j|$, is the most famous one, despite not satisfying oracle properties (see [Fan and Li 2001](#)). A prominent alternative to norm-based penalties like the LASSO is the SCAD ([Fan 1997](#)), defined, for $a > 2$, as

$$\mathcal{P}_\lambda(\beta_j) = \begin{cases} \lambda |\beta_j| & |\beta_j| < \lambda, \\ \frac{(a^2 - 1)\lambda^2 - (|\beta_j| - a\lambda)^2}{2(a - 1)} & \lambda \leq |\beta_j| < a\lambda, \\ \frac{(a + 1)\lambda^2}{2} & |\beta_j| \geq a\lambda. \end{cases} \quad (17)$$

([Fan and Li 2001](#) suggested taking $a = 3.7$) The SCAD satisfies the oracle properties and, in general, improves the features of the LASSO ([Fan and Li 2001](#)). [Aneiros et al. \(2015\)](#) demonstrated the consistency of variable selection achieved using the PeLS procedure combined with the SCAD penalty. They also derived the convergence rates for the estimators and established the oracle property in the context of the SFPLM.

Both penalty functions, LASSO and SCAD, are included in the `fsemipar` package. In fact, the package features a generalization of both penalties. Specifically, it facilitates dealing with grouped partial linear models. In this scenario, the scalar regressors are divided into M groups, denoted as $\mathbf{Z}_{im} = (Z_{im1}, \dots, Z_{imv_m})^\top$ for $m = 1, \dots, M$, where $\sum_{m=1}^M v_m = p_n$. In such situations, the focus is not on selecting variables individually, but rather on choosing important factors, each corresponding to a group of covariates. [Yuan and Lin \(2005\)](#) proposed the group LASSO penalty defined as $P_\lambda(\boldsymbol{\beta}) = \lambda \sum_{m=1}^M \sqrt{\boldsymbol{\beta}_m^\top K_m \boldsymbol{\beta}_m}$, where K_m are positive definite matrices for $m \in 1, \dots, M$. They used $K_m = v_m I_{v_m}$, with $m \in 1, \dots, M$, where I_{v_m} is the identity matrix of dimension v_m . [Wang et al. \(2007\)](#) proposed the group SCAD penalty, defined as $P_\lambda(\boldsymbol{\beta}) = \lambda \sum_{m=1}^M \mathcal{P}_\lambda(\sum_{r=1}^{v_m} \beta_{mr}^2)$, where $\mathcal{P}_\lambda(\cdot)$ was defined in (17). Both group LASSO and group SCAD penalties are included in the `fsemipar` package. It is important to note that when $M = 1$, individual selection is performed.

Another important aspect is the selection of the parameter λ_j ($j = 1, \dots, p_n$) on which the penalty functions depend (see expression (16)). To reduce the number of parameters to select, we consider

$\lambda_j = \lambda \widehat{\sigma}_{\beta_{0,j,OLS}}$, where $\beta_{0,j,OLS}$ denotes the ordinary least-squares (OLS) estimate of $\beta_{0,j}$ and $\widehat{\sigma}_{\beta_{0,j,OLS}}$ is the estimated standard deviation.

Remark 3.1. *Note that in step 1 we must perform nonparametric regression, which involves a tuning parameter, h (kernel) or k (k NN). Therefore we compute the nonparametric fit for a grid of values for the tuning parameter, with each value leading to a different linear model in expression (15). In the package `fsemipar`, the PeLS objective function (16) is minimised using the function `grpreg` of the package `grpreg` (Brehehy and Huang 2015). Specifically, for each linear model (15) (setting the value of h or k), the function `grpreg` fits the regularization path over a grid of values for λ (obtains the value of β that minimises (16) for each λ in the grid). This optimisation is carried out using the coordinate descent approach in Brehehy and Huang (2011). Then, the function `select` (`grpreg` package) is used to determine the optimal value of λ for each linear model using a predefined objective criterion, such as Generalised CV (GCV), k -folds CV or Bayesian Information Criterion (BIC). Finally, the same criterion is used to select the optimal value for \widehat{h} or \widehat{k} . Therefore, once selected the linear model, $\widehat{\lambda}$ is also determined and, as a consequence, we have obtained $\widehat{\beta}_0$. The estimated values \widehat{h} or \widehat{k} and $\widehat{\beta}_0$ are then used in step 3 to fit the nonparametric component of the model.*

Next, we provide the pseudocode for kernel-based SFPLM estimation; k NN-based estimation would be analogous: Novo et al. (2021a) adapted the described procedure to fit the SFPLSIM (13).

Algorithm 1 SFPLM estimation

- 1: **for** each h in the grid **do**
 - 2: Perform functional nonparametric regression to estimate $\mathbb{E}(Y_i|\mathcal{X}_i)$ and $\mathbb{E}(\mathbf{Z}_i|\mathcal{X}_i)$.
 - 3: Denote by $\widehat{m}_h^{y_i}$ and $\widehat{m}_h^{z_i}$ the respective estimates. Obtain $\widetilde{Y}_i = Y_i - \widehat{m}_h^{y_i}$ and $\widetilde{\mathbf{Z}}_i = \mathbf{Z}_i - \widehat{m}_h^{z_i}$.
 - 4: Construct a linear model as in (15).
 - 5: **for** each $\lambda = \lambda_h$ in the grid **do**
 - 6: Use `grpreg` to obtain the $\beta_{h,\lambda}$ that minimises (16). Denote it by $\widehat{\beta}_{h,\lambda}$.
 - 7: **end for**
 - 8: Use `select` to determine the optimal λ_h using with a pre-specified criterion. Denote it by $\widehat{\lambda}_h$.
 - 9: **end for**
 - 10: Use the same criterion to select the optimal h . Denote it by \widehat{h} . Then, $\widehat{\lambda} = \widehat{\lambda}_{\widehat{h}}$ and $\widehat{\beta}_0 = \widehat{\beta}_{\widehat{h},\widehat{\lambda}}$.
 - 11: Perform functional nonparametric regression using \widehat{h} to fit the residuals $Y_i - \mathbf{Z}_i \widehat{\beta}_0$ to obtain $\widehat{m}_{\widehat{h}}$.
-

In this case, conditional expectations in the expression (14) become $\mathbb{E}(Y_i|\mathcal{X}_i) = \mathbb{E}(Y_i|\langle \theta_0, \mathcal{X}_i \rangle)$ and $\mathbb{E}(\mathbf{Z}_i|\mathcal{X}_i) = \mathbb{E}(\mathbf{Z}_i|\langle \theta_0, \mathcal{X}_i \rangle)$, which must be estimated through functional single-index regression. For that we can use either kernel- or k NN-based procedures in expression (5). In the second step, we apply the PeLS procedure, see expression (16), but now the profile least-squares function also depends on θ .

$$\mathcal{Q}(\beta, \theta) = \frac{1}{2} \left(\widetilde{\mathbf{Y}}_\theta - \widetilde{\mathbf{Z}}_\theta \beta \right)^\top \left(\widetilde{\mathbf{Y}}_\theta - \widetilde{\mathbf{Z}}_\theta \beta \right) + n \sum_{j=1}^{p_n} \mathcal{P}_{\lambda_j}(\beta_j). \quad (18)$$

Therefore, the minimisation must be performed over both β and θ . Once $\widehat{\beta}_0$ and $\widehat{\theta}_0$ are obtained, we estimate the real-valued link function r in the same way as $m(\cdot)$ in the SFPLM, but now using one of the expressions in (5). Novo et al. (2021a) demonstrated the consistency of the PeLS procedure with

the SCAD penalty in the context of the SFPLSIM. They also obtained the convergence rates for the estimators and established the oracle property in this setting.

Remark 3.2. *In the case of the SFPLSIM, step 1 involves using functional single-index regression. We follow the procedure in Section 2.2.1 to obtain the set of functional directions Θ . Therefore we compute the nonparametric fit for a grid of values for the tuning parameter (h or k) and for each $\theta \in \Theta$. As a result, each pair (θ, h) or (θ, k) leads to a different linear model in expression (15). For each linear model (15) (setting the values of h or k and θ), the minimisation of expression (16) is carried out using the function `grpreg` over a grid of values for λ . Then, we use the function `select` to determine the optimal value for λ using a predefined objective criterion for each linear model. The same criterion is used to select the optimal value for h or k , therefore we obtain the optimal β for each $\theta \in \Theta$. After that, the $\hat{\theta}_0$ is the $\theta \in \Theta$ that offers a lower value of the objective function $\mathcal{Q}(\cdot, \cdot)$ and \hat{h}/\hat{k} and $\hat{\beta}_0$ the associated optimal values for the remaining parameters. The estimated values \hat{h} or \hat{k} , $\hat{\theta}_0$ and $\hat{\beta}_0$ are then used in step 3 to fit the semiparametric component of the model. As can be observed we perform a joint selection of the tuning parameters of the model, so we must take into account the considerations in Section 2.2.1.*

Next, we provide the pseudocode for kernel-based SFPLSIM estimation; k NN-based estimation would be analogous:

Algorithm 2 SFPLSIM estimation

```

1: for each  $\theta \in \Theta$  do
2:   for each  $h$  in the grid do
3:     Perform functional single-index regression to estimate  $\mathbb{E}(Y_i | \langle \theta, \mathcal{X}_i \rangle)$  and  $\mathbb{E}(\mathbf{Z}_i | \langle \theta, \mathcal{X}_i \rangle)$ .
4:     Denote by  $\hat{r}_{\theta,h}^{y_i}$  and  $\hat{r}_{\theta,h}^{z_i}$  the respective estimates. Obtain  $\tilde{Y}_i = Y_i - \hat{r}_{\theta,h}^{y_i}$  and  $\tilde{\mathbf{Z}}_i = \mathbf{Z}_i - \hat{r}_{\theta,h}^{z_i}$ .
5:     Construct a linear model as in (15).
6:     for each  $\lambda = \lambda_{h,\theta}$  in the grid do
7:       Use grpreg to obtain the  $\beta_{h,\lambda,\theta}$  that minimises (18). Denote it by  $\hat{\beta}_{h,\lambda,\theta}$ .
8:     end for
9:     Use select to determine the optimal  $\lambda_{h,\theta}$  using with a prespecified criterion. Denote it by  $\hat{\lambda}_{h,\theta}$ .
10:  end for
11:  Use the same criterion to select the optimal  $h = h_\theta$ . Denote it by  $\hat{h}_\theta$ .
12: end for
13: Select the  $\theta$  that minimises (18) when  $\beta = \hat{\beta}_{\hat{h}_\theta, \hat{\lambda}_{\hat{h}_\theta, \theta}}$  is considered. Denote it by  $\hat{\theta}_0$ . Then,  $\hat{h} = \hat{h}_{\hat{\theta}_0}$ ,
     $\hat{\lambda} = \hat{\lambda}_{\hat{h}, \hat{\theta}_0}$  and  $\hat{\beta}_0 = \hat{\beta}_{\hat{h}, \hat{\lambda}, \hat{\theta}_0}$ .
14: Perform functional single-index regression using  $\hat{h}$  and  $\hat{\theta}_0$  to fit the residuals  $Y_i - \mathbf{Z}_i \hat{\beta}_0$  to obtain  $\hat{r}_{\hat{h}, \hat{\theta}_0}$ .

```

3.3 Fitting SFPLM and SFPLSIM with the `fsemipar` package

The `fsemipar` package contains functions to estimate the SFPLM and SFPLSIM using the procedures described in Section 3.2. As in the FSIM case, it provides the flexibility to perform both kernel- and

k NN-based fitting. The primary related functions are summarised in the Table 5 along with the corresponding S3 classes designed to include essential S3 methods (`print()`, `summary()`, `plot()` and `predict()`).

Model	Function	S3 class	Description
SFPLM	<code>sfpl.kernel.fit</code>	'sfpl.kernel'	PeLS with kernel estimation.
	<code>sfpl.kNN.fit</code>	'sfpl.kNN'	PeLS with k NN estimation.
SFPLSIM	<code>sfplsim.kernel.fit</code>	'sfplsim.kernel'	PeLS with kernel estimation.
	<code>sfplsim.kNN.fit</code>	'sfplsim.kNN'	PeLS with k NN estimation.

Table 5: Summary of main functions for the SFPLM and SFPLSIM, together with the associated S3 classes.

3.3.1 Main fitting functions

The main fitting functions for the SFPLM and the SFPLSIM (Table 5) share three required arguments:

- The functional predictor \mathbf{x} , a matrix of dimension (n, p) containing n curves discretised in p points
- The scalar covariates \mathbf{z} , a matrix of dimension (n, p_n) .
- The scalar response variable \mathbf{y} , a vector of dimension n .

```
sfpl.kernel.fit(x,z,y,...)
sfpl.kNN.fit(x,z,y,...)
sfplsim.kernel.fit(x,z,y,...)
sfplsim.kNN.fit(x,z,y,...)
```

However, these functions additionally accept numerous optional parameters to provide more precise customisation; some of them have been already introduced in the main fitting functions for the FSIM:

- *Optional arguments for the PeLS procedure.* In this item, we include the arguments related to the penalisation function and the selection of the tuning parameter λ . These arguments are listed in Table 6. The PeLS objective function is minimised using the function `grpreg` of the package `grpreg` (Breheny and Huang 2015). The four functions listed in Table 5 share a default option for constructing the sequence of λ values from which $\hat{\lambda}$ will be chosen. This sequence is generated by starting from a minimum value (expressed as a fraction of the maximum value) controlled by the user, and it can contain a customisable number of values. More specifically, the user has the option to specify a value for the minimum λ to face two different situations: when n is smaller than `factor.pn` (default 1) times p_n , this value can be set using the `lambda.min.h` argument (default 0.05); when n is greater, the `lambda.min.1` argument (default 0.00001) allows the user to set a different value. The utility of these options will be showed in Sections 4.3.2 and 4.3.3. Alternatively, we can directly specify a unique value for the minimum lambda using the

`lambda.min` argument. When `lambda.min` is provided, `lambda.min.h` and `lambda.min.l` are disregarded. Furthermore, the number of λ values in the sequence can be customized using the `nlambda` argument (default 100). Additionally, the user has the option to provide the sequence of λ values directly through the `lambda.seq` argument. When `lambda.seq` is provided, all of the previously mentioned arguments are ignored. Note that setting `lambda.seq` to 0 results in non-penalized fitting, which corresponds to the ordinary least-squares estimates.

In addition, we can choose the criterion to select λ and the tuning parameter h (kernel-based functions) or k (kNN-based functions). This can be done through the argument `criterion` (default "GCV") and the available options are "GCV", "AIC", "BIC" and "k-fold-CV". If we choose k -fold CV, we can specify the number of CV folds using `nfolds` (default 10) and also set the seed to obtain reproducible results using the argument `seed` (default 123).

The functions listed in Table 5 also allow for grouped variable selection. Using the argument `vn` (default `vn=ncol(z)`, which leads to individual penalisation), the user can directly specify the number of groups or to provide a vector of possibilities so that the routines select the optimal number of groups according to the provided `criterion`. For instance, $v_n = p_n$ means that each variable is a group (ungrouped case); whereas `vn=c(pn,2)` means that routines will choose between the ungrouped case and the case with two groups of consecutive variables (both of size $n/2$, if n is even).

Finally, the user can also choose between the penalty function SCAD/group SCAD (`grSCAD`) and LASSO/group LASSO (`grLASSO`) using the argument `penalty` (default `grSCAD`), and set the maximum number of iterations over each regularisation path through the argument `max.iter` (default 1000).

- *Optional arguments for the nonparametric fit.* This item refers to the arguments that are collected in Table 2. Functions that perform the kernel-based procedure accept the same arguments as `fsim.kernel.fit()` and `fsim.kernel.fit.optim()`. Similarly, functions implementing the k NN-based estimation accept arguments consistent with `fsim.kNN.fit()` and `fsim.kNN.fit.optim()`. The four functions in Table 5 accept the argument `kind.of.kernel`. Additionally, the functions for the SFPLM allow the choice of the semimetric using the argument `semimetric` (default "deriv"). Currently, only the semimetric based on the B-spline representation of derivatives, `semimetric="deriv"`, and the based on FPCA, `semimetric="pca"`, are implemented. The code of these functions is based on the Frederic Ferraty routines included in the web page <https://www.math.univ-toulouse.fr/~ferraty/SOFTWARES/NPFDA/index.html>. If `semimetric="deriv"`, the argument `q` allows the user to control the order of the derivative (default `q=0`). If `semimetric="pca"`, the argument `q` controls the number of principal components retained (default `q=2`).
- *Optional arguments for B-spline expansions.* Functions for the SFPLSIM allow all the arguments listed in Table 3; functions for the SFPLM, only those related to the B-spline expansion of the curves (`order.Bspline`, `nknot` and `range.grid`).
- *Optional arguments for the parallel computation.* The functions for the SFPLSIM, which are time consuming in contrast to functions for the SFPLM, allow for parallel computation. Similar

Function	Argument	Description
	<code>lambda.min.h</code>	Smallest value for λ if <code>n<factor.pn*pn</code> .
	<code>lambda.min.l</code>	Smallest value for λ if <code>n>factor.pn*pn</code> .
	<code>lambda.min</code>	Smallest value for λ .
	<code>factor.pn</code>	Positive integer used to set the smallest value for λ .
<code>sfpl.kernel.fit</code>	<code>nlambda</code>	Number of λ values in the sequence.
<code>sfpl.kNN.fit</code>	<code>lambda.seq</code>	Sequence of λ values.
<code>sfplsim.kernel.fit</code>	<code>vn</code>	Integer/vector of integers indicating the number/numbers of groups of variables to be penalised together.
<code>sfplsim.kNN.fit</code>	<code>criterion</code>	Criterion for selecting $\hat{\lambda}$ and \hat{h}/\hat{k} : "GCV", "BIC", "AIC", "k-fold-CV".
	<code>nfolds</code>	If <code>criterion= "k-fold-CV"</code> : number of CV folds.
	<code>seed</code>	If <code>criterion= "k-fold-CV"</code> : Seed to obtain reproducible results.
	<code>penalty</code>	Penalty function: "grLASSO", "grSCAD".
	<code>max.iter</code>	Maximum number of iterations (across the entire path).

Table 6: Optional input arguments related to the PeLS procedure.

to the FSIM functions, the user can specify the number of CPU cores to use for parallel execution by setting the argument `n.core` (see the item *Optional arguments for the parallel computation* in Section 2.3.1).

3.3.2 Case study I, part II: Tecator dataset

In [Novo et al. \(2021a\)](#), the authors studied the inclusion of protein and moisture content as covariates to predict the fat content in each piece of meat. They also investigated whether the quadratic, cubic, and interaction effects of these scalar covariates should be included in the model. This means to consider initially seven scalar covariates: denoting by Z_1 and Z_2 the protein and moisture contents, respectively, they considered as linear covariates $Z_{2j-1} = Z_1^j$ and $Z_{2j} = Z_2^j$ (for $j = 1, 2, 3$), and $Z_7 = Z_1 Z_2$. They fitted both an SFPLM and an SFPLSIM to the data, using PeLS estimation with a SCAD penalty combined with a kernel-based technique. In addition, they used the BIC criterion for selecting the tuning parameters. In this context, we can illustrate and compare functions in Table 5 by extending that application, thereby demonstrating the wide range of capabilities of the `fsemipar` package.

As an example, the following code shows the implementation of the SFPLSIM using the function `sfplsim.kernel.fit()`. In addition to the data, we have provided some specific input arguments to improve the fit: we have reduced the interval in which the bandwidth is selected (setting `max.q.h=0.35`) discarding the largest values (given that by default `num.h=10`, reducing these interval

will lead to more precision in the selection of \hat{h} without increasing the computational cost), we have also increased the minimum value of the sequence for selecting λ (`lambda.min=0.01`) and the number of iterations (`max.iter=5000`) trying to avoid convergence problems in this context of high dependence between predictors; we also chose the BIC as the criterion for selecting the tuning parameters, which leads to slightly faster computation than GCV. As in Section 2.3.2, we set `nknot.theta=4`, `nknot=20` and `range.grid=c(850,1050)`.

```
>z1<-Tecator$protein
>z2<-Tecator$moisture
>z.com<-cbind(z1,z2,z1^2,z2^2,z1^3,z2^3,z1*z2)
>fit2<-sfplsim.kernel.fit(x=x[train,], z=z.com[train,], y=y[train],
max.q.h=0.35,lambda.min.l=0.01,max.iter=5000, nknot.theta=4,criterion="BIC",
nknot=20,range.grid=c(850,1050))
```

The fitted object resulting from the functions listed in Table 5 contains valuable information about the performed estimation. This includes the fitted values for the response (`fitted.values`), the residuals (`residuals`), and the estimates for the linear coefficients (`beta.est`). It also provides the selected values for the tuning parameters, such as \hat{h} (`h.opt`) or \hat{k} (`k.opt`), and $\hat{\lambda}$ (`lambda.opt`). Additionally, the object includes the optimal value of the criterion used to select \hat{h}/\hat{k} and $\hat{\lambda}$ (IC), as well as the optimal value of the objective function of the PeLS procedure (see 16) (Q). In the case of SFPLSIM, it also contains the coefficients of $\hat{\theta}$ in the B-spline basis (`theta.est`), among other details.

In the case of `sfplsim.kernel.fit()` (class `sfplsim.kernel`), the fitted object can be used in the functions `print.sfplsim.kernel()` and `summary.sfplsim.kernel()` to display summaries of the fitted model. It can also be used in `predict.sfplsim.kernel()` to obtain predictions for new values of the covariates provided by the arguments `newdata.x` (curves) and `newdata.z` (scalar predictors). This function implements two possibilities for prediction:

- If `option=1`, we maintain all the estimations (`h.opt`, `beta.est` and `theta.est`) to predict the functional single-index component of the model.
- If `option=2`, we maintain `beta.est` and `theta.est`, while the tuning parameter (`h.opt`) is selected again to predict the functional single-index component of the model. This selection is performed using the LOOCV criterion in the associated FSIM.

For each option, the MSE_P is also obtained when the user provides the actual responses via the `y.test` argument. The remaining functions of Table 5 offer analogous possibilities for prediction.

```
> summary(fit2)
*** SFPLSIM fitted using penalized least-squares combined with kernel estimation with
Nadaraya-Watson weights ***

-Call: sfplsim.kernel.fit(x = x[train, ], z = z.com[train, ], y = y[train],
nknot.theta = 4, max.q.h = 0.35, range.grid = c(850, 1050), nknot = 20,
lambda.min= 0.01, criterion = "BIC", max.iter = 5000)
```

```

-Bandwidth (h): 27.11844
-Theta coefficients in the B-spline basis: 0.1656316 -0.1656316 0 0.1656316 -0.1656316
0 0.1656316
-Linear coefficients (beta): 0.6852112 -1.98299 0 0.01086126 -0.001282229 0 0
-Number of non-zero linear coefficients: 4
-Indexes non-zero beta-coefficients: 1 2 4 5
-Lambda: 0.01244154
-IC: 523.0534
-Q: 102.0231
-Penalty: grSCAD
-Criterion: BIC
-vn: 7

```

```

> predict(fit2,newdata.x=x[161:215,],newdata.z=z.com[161:215,],y.test=y[161:215],
option=2)$MSEP
[1] 1.262723

```

Regarding the prediction, Table 7 displays the MSEP and selected scalar covariates corresponding to each primary fitting function when using the respective BIC selectors for n_r (only in the SFPSLIM), λ , and h , or k . In the functions for the SFPLM, the results were obtained using the semimetric based on the derivatives (`semimetric="deriv"`, the option by default) and as \mathbf{x} contains already the second derivative of the curves, we used the option `q=0` (also, the option by default).

```

sfpl.knn<-sfpl.knn.fit(x=x[train,],y=y[train],z=z.com[train,], step=1, min.knn=10,
max.knn=15,criterion="BIC",range.grid=c(850,1050),lambda.min=0.01,nknot=20,max.iter=
5000)

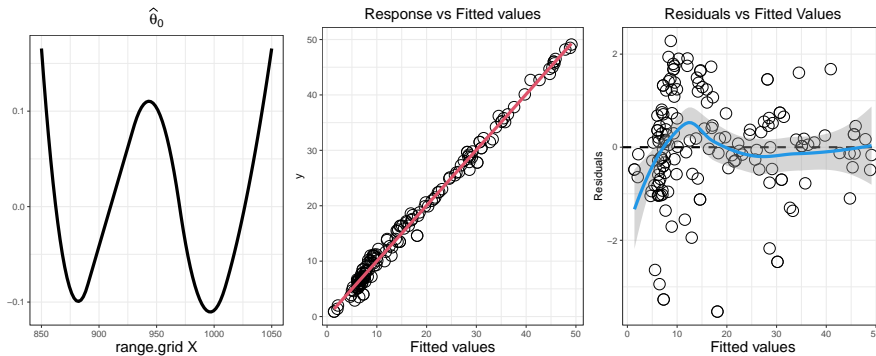
```

As can be observed from Table 7, under the conditions described, the best result in MSEP is obtained with the SFPLM estimated using PeLS with k NN estimation, which retains only 3 scalar covariates in the model. Finally, the output of the S3 method `plot()` for the functions in Table 5 represents two

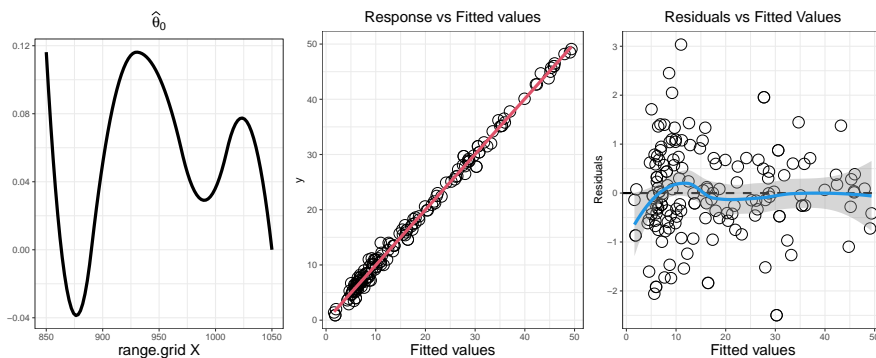
Function	Selected variables	\hat{n}_r	MSEP	
			1	2
<code>sfpl.kernel.fit()</code>	Z_1, Z_2	-	1.317	1.317
<code>sfpl.knn.fit()</code>	Z_2, Z_3, Z_4	-	0.797	0.797
<code>sfplsim.kernel.fit()</code>	Z_1, Z_2, Z_4, Z_5	4	1.260	1.263
<code>sfplsim.knn.fit()</code>	Z_1, Z_2, Z_3, Z_4	4	1.349	1.349

Table 7: MSEP obtained for each function using the respective BIC selectors for tuning parameters (h/k , λ ; also n_r in the SFPLSIM fitting functions).

diagnostic plots in addition to the estimated functional index for the SFPLSIM fitting functions. In Figures 4 and 5, we provide the outputs of the 4 main functions, obtained under the same conditions as Table 7.



(a) `sfplsim.kernel.fit()` ($\hat{n}_r = 4$)



(b) `sfplsim.kNN.fit()` ($\hat{n}_r^* = 4$)

Figure 4: Outputs of the S3 method `plot()` applied to the fitted objects of functions for the SFPLSIM, using the corresponding BIC selectors for the tuning parameters and n_r .

4 Multiple scalar predictors with functional origin and a functional covariate

In Section 4, we focus on SoF regression including as predictors multiple scalar variables with linear effect coming from the discretisation of a curve. Section 4.1 introduces the concept of *points of impact* and some modelling alternatives based on linear or partial linear approaches when more than one functional variable is available. In Section 4.2, we discuss the techniques implemented in `fsemipar` for estimation and selection of points of impact in such models. In Section 4.3 we present the associated functions of the package and illustrate their use through two real chemometric datasets.

4.1 Linear and partial linear modelling approaches

In several studies, the interpretability of the outcomes prompted researchers to revisit the concept of discretising functional objects. They discovered that the discretised values of a random curve $\zeta(t)$, $\zeta(t_1), \dots, \zeta(t_{p_n})$, might hold insights that are not accessible via the continuous curve $\zeta(t)$, and vice versa (see, for instance, [McKeague and Sen 2010](#)). So, in certain applications we want to sift through the discretised observations of a curve $\zeta(t)$ and identify the points of the domain at which the curve most influence a scalar variable of interest Y . In some papers (for example, [Kneip et al. 2016](#) or [Novo](#)

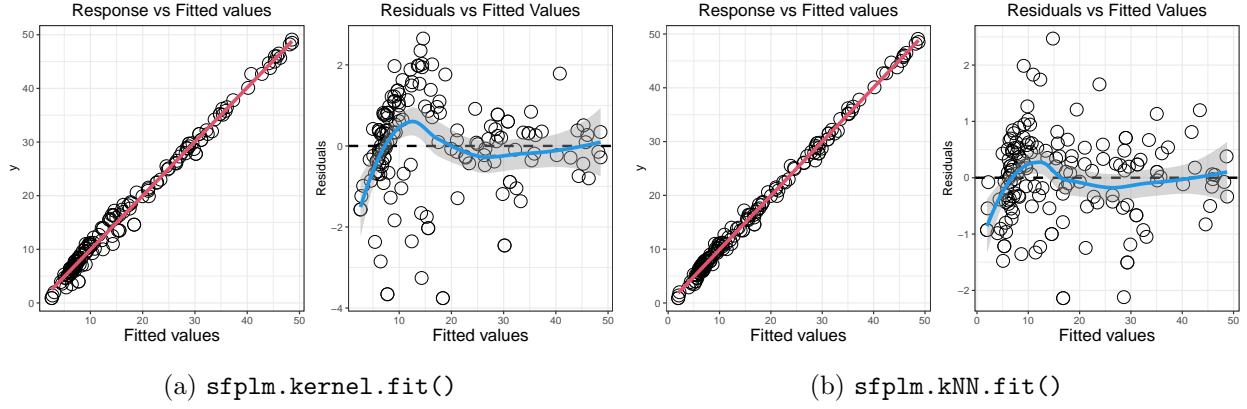


Figure 5: Outputs of the S3 method `plot()` applied to the fitted objects of functions for the SFPLM, using the corresponding BIC selectors for the tuning parameters.

[et al. 2021b](#), among others), these points of the domain are called *points of impact*, so we will follow such terminology along the paper. In the following lines, we summarise the modelling alternatives involving the discretised values of a curve (scalar variables with functional origin) implemented in the package `fsemipar`:

- The multiple linear model (MLM) studied in [Aneiros and Vieu \(2014\)](#), which is given by the expression:

$$Y_i = \beta_{00} + \sum_{j=1}^{p_n} \beta_{0j} \zeta_i(t_j) + \varepsilon_i, \quad i = 1, \dots, n, \quad (19)$$

where ζ_i is a random curve defined on some interval $[a, b]$ and is observed in the points $a \leq t_1 < \dots < t_{p_n} \leq b$. In addition, $(\beta_{00}, \beta_{01}, \dots, \beta_{0p_n})^\top$ is a vector of unknown real coefficients.

- The multi-functional partial linear model (MFPLM) examined in [Aneiros and Vieu \(2015\)](#). This model follows the expression

$$Y_i = \sum_{j=1}^{p_n} \beta_{0j} \zeta_i(t_j) + m(\mathcal{X}_i) + \varepsilon_i, \quad i = 1, \dots, n, \quad (20)$$

where \mathcal{X}_i denotes another functional variable valued in some semi-metric space, which influences the response nonparametrically.

- The multi-functional partial linear single-index model (MFPLSIM) studied in [Novo et al. \(2021b\)](#), defined by the following relationship:

$$Y_i = \sum_{j=1}^{p_n} \beta_{0j} \zeta_i(t_j) + r(\langle \theta_0, \mathcal{X}_i \rangle) + \varepsilon_i \quad i = 1, \dots, n. \quad (21)$$

Here, \mathcal{X}_i is valued in a separable Hilbert space and its effect on the response is given through a functional single-index component.

In models (19)-(21), it is assumed that $p_n \rightarrow \infty$ as $n \rightarrow \infty$, and only a few of the discretised points $\zeta(t_j)$, $j = 1, \dots, p_n$, influence the response Y . We could consider applying to these models the same

techniques described in Section 3.2 to estimate and select relevant variables in the linear component. However, these methods are often inadequate for two main reasons. First, there exists a strong dependence between variables, a consequence of their functional origin. Second, the sheer number of observations ($n \ll p_n$) makes it difficult to obtain results in a reasonable time frame. Then, it is necessary to develop specialised methods tailored to these particular scenarios. Therefore, in the following section, we provide a short review of the techniques implemented in `fsemipar` for estimating these models.

4.2 Selection of points of impact and model estimation

Aneiros and Vieu (2014) proposed an algorithm called Partitioning Variable Selection (PVS) for the MLM (19). This two-step procedure is based on the idea that observations $\zeta_i(t_j)$ and $\zeta_i(t_k)$, where t_j and t_k are closely spaced points in the domain of the curve, contain similar information about the response. The method proceeds as follows:

1. In the first step, it considers a reduced linear model incorporating only a few covariates, w_n , covering the entire discretisation interval of $\zeta_i(t)$. For this purpose:
 - We assume, without loss of generality, that $p_n = q_n w_n$.
 - The w_n variables taken into account are $\zeta_i(t_{(2k-1)q_n/2})$ with $k \in \{1, \dots, w_n\}$.
 - The remaining $p_n - w_n$ covariates from the original set are directly discarded.

A PeLS procedure (see Section 3.2) is applied to the reduced model. In this manner, the dependence among covariates is mitigated before the variable selection is performed.

2. In the second step, a linear model is considered that includes the variables selected in the first step and those in their neighbourhood. Specifically:
 - Let's denote $\widehat{S}_{1n} = \{k = 1, \dots, w_n, \widehat{\beta}_{(2k-1)q_n/2} \neq 0\}$.
 - The set of covariates considered in the second step is

$$\mathcal{R} = \cup_{k \in \widehat{S}_{1n}} \{\zeta_i(t_{(k-1)q_n+1}), \zeta_i(t_{(k-1)q_n+2}) \dots, \zeta_i(t_{kq_n})\}.$$

A PeLS procedure is applied again to the resultant model. By doing so, relevant information that may have been overlooked in the first step is reconsidered.

The outputs of the second step of the PVS algorithm are the estimates for the MLM (19). The selected points of impact are those belonging to the set $\widehat{S}_{2n} = \{j = 1, \dots, p_n, \text{ such that } \zeta_i(t_j) \in \mathcal{R} \text{ and } \widehat{\beta}_{0j} \neq 0 \text{ in the second step}\}$, and $\widehat{\beta}_{0j}$ is the estimate of the second step if $\zeta_i(t_j) \in \mathcal{R}$ and 0 otherwise. The PVS algorithm requires dividing the sample to execute the two steps. The natural choice involves using half of the sample in the first step and the other half in the second step, that is $n_1 = n_2 = n/2$, although in some applications this may not be the optimal option. The consistency of this procedure was showed in Aneiros and Vieu (2014), who also provided the rates of convergence of the estimators.

Note that the PVS algorithm has an extra tuning parameter: the number of covariates in the reduced model, w_n , in the first step of the method. This parameter can be selected using the same objective criterion to select the parameter λ in the PeLS procedure involved.

In addition, the first step of the PVS algorithm relies on the assumption $p_n = w_n q_n$. When this assumption fails, we can use the solution proposed by [Aneiros and Vieu \(2015\)](#), which is based on consider non-fixed $q_n = q_{n,k}$ values (for $k = 1, \dots, w_n$) when p_n/w_n is not an integer number. Specifically:

$$q_{n,k} = \begin{cases} [p_n/w_n] + 1 & k \in \{1, \dots, p_n - w_n[p_n/w_n]\}, \\ [p_n/w_n] & k \in \{p_n - w_n[p_n/w_n] + 1, \dots, w_n\}, \end{cases}$$

where $[z]$ denotes the integer part of $z \in \mathbb{R}$.

[Aneiros and Vieu \(2015\)](#) extended the PVS algorithm to estimate the MFPLM (20). The idea was to transform the MFPLM (20) into a linear model using the same strategy described in Section 3.2. Once an approximate linear model was obtained, they applied the PVS algorithm to that model. They proved the consistency of the method and obtained the rates of convergence for the estimators.

[Novo et al. \(2021b\)](#) addressed the MFPLSIM (21). In this case, there were two additional challenges when extending the PVS: first, estimating the functional index θ_0 was computationally intensive, and second, it required a relatively large sample size (see [Aneiros et al. 2022](#)). They then explored two variants of the PVS algorithm: the improved algorithm for sparse multi-functional regression (IASSMR), which essentially adapts the PVS to the MFPLSIM, and the fast algorithm for sparse multi-functional regression (FASSMR), which employs only the first step of the PVS. The motivation for the latter variant was to reduce the computational cost for large discretisation sizes (p_n) and improve performance in situations with small sample sizes, as the sample no longer needs to be divided. Both the IASSMR and the FASSMR require the transformation of the expression (21) into a linear model, using the strategy described in Section 3.2. In [Novo et al. \(2021b\)](#), the authors demonstrated the consistency of both methods and derived the convergence rates for the estimators of the former.

4.3 Fitting the MLM, MFPLM and MFPLSIM with the `fsemipar` package

The `fsemipar` package implements the algorithms described in Section 4.2 to estimate models (19)-(21). In the case of models with partial linear structure, it provides the flexibility to perform both kernel- and k NN-based fitting. The primary related functions are summarised in the Table 8 along with the corresponding S3 classes.

Model	Function	S3 class	Description
MLM	<code>PVS.fit</code>	'PVS'	PVS algorithm.
MFPLM	<code>PVS.kernel.fit</code>	'PVS.kernel'	PVS algorithm with kernel estimation.
	<code>PVS.kNN.fit</code>	'PVS.kNN'	PVS algorithm with k NN estimation.
MFPLSIM	<code>IASSMR.kernel.fit</code>	'IASSMR.kernel'	IASSMR with kernel estimation.
	<code>IASSMR.kNN.fit</code>	'IASSMR.kNN'	IASSMR with k NN estimation.
	<code>FASSMR.kernel.fit</code>	'FASSMR.kernel'	FASSMR with kernel estimation.
	<code>FASSMR.kNN.fit</code>	'FASSMR.kNN'	FASSMR with k NN estimation.

Table 8: Summary of main functions for MLM, MFPLM and MFPLSIM together with the associated S3 classes.

4.3.1 Main fitting functions

The main fitting functions for MLM, MFPLM and MFPLSIM (Table 8) share the following required arguments:

- The functional predictor \mathbf{z} (pointwise effect), a matrix of dimension (n, p_n) containing n curves discretised in p_n points.
- The scalar response variable \mathbf{y} , a vector of dimension n .

```
PVS.fit(z,y,...)
```

In the case of the MFPLM and MFPLSIM, the functions also require:

- The functional predictor \mathbf{x} (continuous effect), a matrix of dimension (n, p) containing n curves discretised in p points.

```
PVS.kernel.fit(x,z,y,...)
```

```
PVS.kNN.fit(x,z,y,...)
```

```
IASSMR.kernel.fit(x,z,y,...)
```

```
IASSMR.kNN.fit(x,z,y,...)
```

```
FASSMR.kernel.fit(x,z,y,...)
```

```
FASSMR.kNN.fit(x,z,y,...)
```

These functions additionally accept numerous optional parameters. Many of them have been already introduced in Section 3.3.1:

- *Optional arguments for the two steps of the algorithm.* In functions tailored to PVS and IASSMR (which are two-step procedures), users can control the indices of the data used for the first and second steps with the arguments `train.1` (default `1:ceiling(n/2)`) and `train.2` (default `(ceiling(n/2)+1):n`), respectively. Additionally, for the seven functions listed in Table 8, the argument `wn` (default `c(10,15,20)`) allows users to provide a sequence of possible values for w_n in the reduced model of step 1.
- *Optional arguments for the PeLS procedure.* These arguments are listed in Table 6 and commented in Section 3.3.1. In this case, the `criterion` chosen by the user to select the tuning parameters of the estimation/variable selection procedure is also used to select \hat{w}_n from the values provided in `wn`.

In addition, functions related to the MFPLM and MFPLSIM admit the following optional arguments:

- *Optional arguments for the nonparametric fit.* This item refers to the arguments collected in Table 2. Kernel-based functions accept the same arguments as `fsim.kernel.fit()` and `fsim.kernel.fit.optim()`, and k NN-based ones accept arguments consistent with `fsim.kNN.fit()` and `fsim.kNN.fit.optim()`. Additionally, the functions for the MFPLM admit the arguments `semimetric` and `q` (see *Optional arguments for the nonparametric fit* in Section 3.3.1).

- *Optional arguments for B-spline expansions.* Functions for the MFPLSIM allow all the arguments listed in Table 3; functions for the MFPLM, only those related to the B-spline expansion of the curves (`order.Bspline`, `nknot` and `range.grid`).
- *Optional arguments for the parallel computation.* The functions for the MFPLSIM allow for parallel computation, so they admit the argument `n.core` (see the item *Optional arguments for the parallel computation* in Section 2.3.1).

4.3.2 Case study I, part III: Tecator dataset

The purpose of this section is twofold: to illustrate the implementation of the models (19)–(21) using the functions in Table 8 and to show the predictive advantage of including impact points in the modelling of the Tecator dataset.

Although MFPLM (20) (so as to the MFPLSIM (21)) is tailored to address situations with more than one functional covariate, in Aneiros and Vieu (2015), the authors applied it in the case $\zeta(t) = \mathcal{X}(t)$. They model the Tecator dataset (one functional covariate) using the model:

$$Y_i = \sum_{j=1}^{100} \beta_{0j} \mathcal{X}_i(t_j) + m(\mathcal{X}_i) + \varepsilon_i, \quad i = 1, \dots, 160,$$

where \mathcal{X}_i is the second derivative of the absorbance spectrum of each piece of meat, which was recorded in 100 equally spaced wavelengths in the interval 850-1050. To illustrate and compare the functions in Table 8, we extended that application, fitting also the models:

$$Y_i = \sum_{j=1}^{100} \beta_{0j} \mathcal{X}_i(t_j) + r(\langle \mathcal{X}_i, \theta_0 \rangle) + \varepsilon_i, \quad i = 1, \dots, 160.$$

$$Y_i = \beta_{00} + \sum_{j=1}^{100} \beta_{0j} \mathcal{X}_i(t_j) + \varepsilon_i, \quad i = 1, \dots, 160.$$

As an example, the following code shows the implementation of the MFPLSIM using the functions `FASSMR.kernel.fit()` and `IASSMR.kernel.fit()`. In addition to the data, we have provided some specific input arguments. Following the comments made in Section 3.3.2, we set `max.q.h=0.35`, `criterion="BIC"`, `nknot.theta=4`, `nknot=20`, and `range.grid=c(850,1050)`. We increased the smallest value in the sequence to select $\hat{\lambda}$ (`lambda.min=0.03`), trying to obtain a simpler model. Note that in this case, if we use half of the sample in each stage of the two-step procedures (that is, $n_1 = n_2 = 80$ by setting `train.1=1:80` and `train.2=81:160`), then $n_1 > w_n$ and n_2 is likely to exceed the cardinality of \mathcal{R} . Consequently, it may not be worthwhile to specify `lambda.min.h`, `lambda.min.l`, and `factor.pn` (refer to *Optional Arguments for the PeLS Procedure* in Section 3.3.1) to adjust the level of penalization in each step of the IASSMR. Typically, we assign a value to `factor.pn` that is ≥ 1 , aiming to impose greater penalization in situations where the sample size is smaller than the number of covariates in the model.

```
fit3 <- FASSMR.kernel.fit(x=x[train,],z=x[train,], y=y[train], nknot.theta=4,
max.q.h=0.35, range.grid=c(850,1050), nknot=20,criterion="BIC", lambda.min=0.03)
```

```
fit4<- IASSMR.kernel.fit(x=x[train,],z=x[train,], y=y[train],train.1=1:80,train.2=81:160,
nknot.theta=4,max.q.h=0.35, range.grid=c(850,1050), nknot=20,criterion="BIC",
lambda.min=0.03)
```

The objects `fit3` and `fit4` belong to an S3 class (see Table 8), which implements S3 methods. In addition to the information listed in Section 3.3.2, these objects include the selected value for \hat{w}_n (`w.opt`). As in the Sections 2.3.2 and 3.3.2, we can display a summary of the fitted models using `summary.FASSMR.kernel()` (or `print.FASSMR.kernel()`) and `summary.IASSMR.kernel()` (or `print.IASSMR.kernel()`), respectively. To make predictions for the fitted object `fit3`, we can use `predict.FASSMR.kernel()`. This function implements the two possibilities for prediction outlined in Section 3.3.2. To make predictions for `fit4`, we can use `predict.IASSMR.kernel()`, which offers the following possibilities:

- If `option=1`, we retain all the estimates (`h.opt`, `theta.est`, and `beta.est`) to predict the functional single-index component of the model. Since we use the estimates from the second step of the algorithm, only `train.2` was used as the training sample for prediction. Therefore, `h.opt` might not be suitable for predicting the functional single-index component of the model.
- If `option=2`, we keep `theta.est` and `beta.est`, while the tuning parameter \hat{h} is selected anew for predicting the functional single-index component of the model. This selection is performed using the LOOCV criterion in the associated FSIM and the complete training sample (i.e., `train=c(train.1,train.2)`).
- If `option=3`, we maintain only the indices of the relevant variables selected by the IASSMR. We re-estimate the linear coefficients and the functional index using `sfplsim.kernel.fit`, without penalization (by setting `lambda.seq=0`) and using the entire training sample (`train=c(train.1,train.2)`). This method provides two predictions (and MSEPs):
 - a) The prediction associated with `option=1` for the `sfplsim.kernel` class.
 - b) The prediction associated with `option=2` for the `sfplsim.kernel` class.

Note that the objects resulting from the functions `IASSMR.kNN.fit`, `PVS.kernel.fit` and `PVS.kNN.fit` offer analogous possibilities for prediction. For more details, see Section 4.3.3 or refer to the manual of the `fsemipar` package (Aneiros and Novo 2024).

Table 9 displays the MSEP and the selected points of impact for each primary fitting function, using the respective BIC selectors for λ , w_n , and h/k in the MFPLM and MFPLSIM models. The points of impact, selected from the original set of 100, are represented in red on a timeline for enhanced visualization and comparison. The column \hat{s}_n indicates the number of points of impact selected by each function. For the MFPLM functions, the results were obtained using `semimetric="deriv"`. For comparative purposes, the same values for common input arguments were used across the seven functions in Table 8. Additionally, h and k were selected using the same grid for each pair of functions employing kernel/ k NN estimation, setting `min.knn=2`, `max.knn=10`, and `step=1` in the k NN case.

It is remarkable that the MLM does not offer good predictive power in this case. This could be expected since the relationship between the response and the predictor is non-linear, as pointed out in Novo et al. (2019), among others. Another important observation is that the MFPLSIM appears

to offer the lowest MSEP under our conditions, although the MFPLM, estimated using the PVS with k NN smoothing, is also competitive in terms of MSEP. Among the algorithms for estimating the MFPLSIM, it is important to note that even the 1-step procedure offers a very competitive result, especially when combined with kernel estimation. In the two-step procedures, estimating again the tuning parameters (`option=3`) offers the higher predictive power.

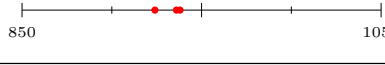

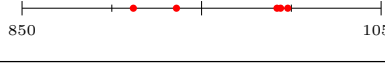
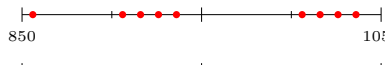
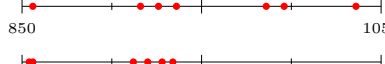
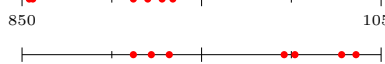

Model	Function	Points of impact	\hat{s}_n	MSEP			
				1	2	3a	3b
MLM	<code>PVS.fit()</code>		3	19.46	-	-	-
MFPLM	<code>PVS.kernel.fit()</code>		7	6.94	5.14	4.66	4.66
	<code>PVS.kNN.fit()</code>		5	2.65	1.84	1.29	1.29
MFPLSIM	<code>FASSMR.kernel.fit()</code>		9	1.60	1.79	-	-
	<code>FASSMR.kNN.fit()</code>		7	2.25	2.25	-	-
	<code>IASSMR.kernel.fit()</code>		6	1.66	1.69	1.10	1.15
	<code>IASSMR.kNN.fit()</code>		7	1.50	1.66	1.04	1.04

Table 9: MSEP obtained for each function using the respective BIC selectors for the tuning parameters (λ and w_n ; also h or k in models with functional nonparametric/single-index component).

Focusing on the selection of impact points, we observe four distinct clusters of impact points. It seems that all algorithms consistently select observations in the second quartile of the timeline (wavelengths between 900 and 950 nm). Additionally, some algorithms select impact points at the beginning of the first quartile, while others choose them at the end of the fourth quartile. Another subset of algorithms selects points towards the end of the third quartile. If we combine this information with the MSEP, the best choice appears to be made by the functions `IASSMR.kNN.fit()` and `IASSMR.kernel.fit()`.

A comparison of Tables 4, 7, and 9 reveals that the lowest MSEP value is obtained when the protein and moisture contents are included in the model (using the SFPLM estimated using `sfpl.kNN.fit()`). However, acquiring these measurements necessitates chemical analyses of the meat samples, which we aim to circumvent by utilizing spectrometric information. A comparison between Table 4 and Table 9 clearly demonstrates that incorporating both continuous and pointwise effects of the functional predictor not only enhances predictive power but also preserves interpretability: each variable is associated with an interpretable parameter in the model.

Finally, the output of the S3 method `plot()` for the functions in Table 8 represents the curves with their impact points (in dashed vertical lines), the same two diagnostic plots as the functions of Section 3.3, and the estimated functional index for the MFPLSIM fitting functions. In Figure 6, we provide the outputs of the 7 main functions (indicating `option=1` to get just the first plot), obtained under the same conditions as Table 9.

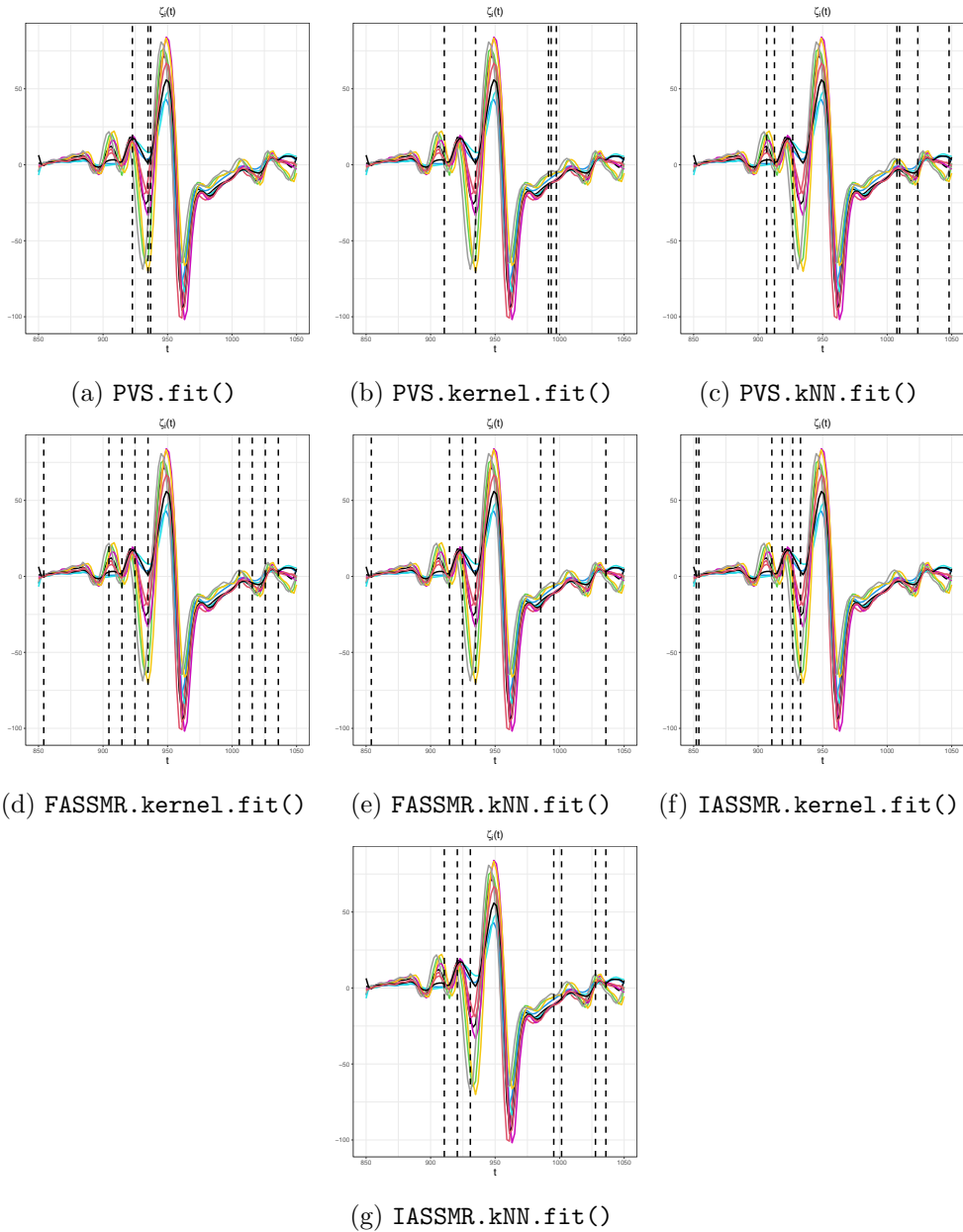


Figure 6: Outputs of the S3 method `plot()` applied to the fitted objects of functions for the MLM, MFPLM and MFPLSIM, using the corresponding BIC selectors for the tuning parameters.

4.3.3 Case study II: Sugar dataset

The purpose of this section is to demonstrate the implementation of the models (20) and (21) when dealing with two functional covariates. Additionally, it addresses scenarios where the discretisation size may exceed the sample size in the second step of the algorithms.

The Sugar dataset contains information about 268 samples obtained at a sugar plant in Scandinavia (see <https://ucphchemometrics.com/sugar-process-data/> for details). For each sample, the absorbance spectra from 275 nm to 560 nm were measured in 0.5 nm intervals ($p_n = 571$). But in this case, unlike Tecator dataset, measurements at several different excitation wavelengths were recorded, generating various functional variables. In this application, we are going to consider two, those taken

into account in Novo et al. (2021b): the absorbance spectra at excitation wavelengths 240 nm (the first functional variable, which will be denoted as ζ) and at excitation wavelengths 290 nm (the second functional variable, which will be named \mathcal{X}). Figure 7 shows a sample of 20 curves from each functional variable.

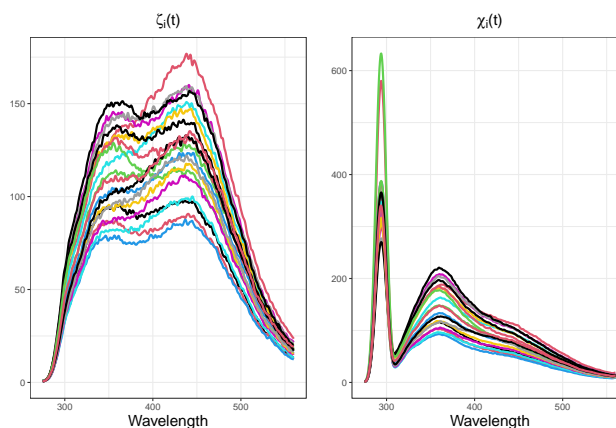


Figure 7: Sample of 20 spectrometric curves measured at excitation wavelengths 240 nm (left panel) and 290 nm (right panel).

In addition, Sugar dataset also contains the ash content of sugar. The target of the statistical analysis is to predict the ash content of sugar having the measurements of the absorbance spectra at those two excitation wavelengths. For that, we used models (20) and (21). In the bi-functional models, to select the most accurate effect of each functional predictor, continuous or pointwise-linear, we followed the study performed in Novo et al. (2021b). They concluded that the absorbance spectra at excitation wavelengths 240 nm ($\zeta(t)$) should be included with the pointwise-linear effect. Then, we fitted models

$$Y_i = \sum_{j=1}^{571} \beta_{0j} \zeta_i(t_j) + m(\mathcal{X}_i) + \varepsilon_i, \quad i = 1, \dots, 216,$$

and

$$Y_i = \sum_{j=1}^{571} \beta_{0j} \zeta_i(t_j) + r(\langle \mathcal{X}_i, \theta_0 \rangle) + \varepsilon_i, \quad i = 1, \dots, 216.$$

From the original set of 268 samples, 2 were discarded as extreme outliers. As a consequence, the available sample size is 266. To compare procedures we split the sample into two subsamples: a training sample composed of the first $n = 216$ observations and a testing sample containing the $n_{test} = 50$ last.

```
>data(Sugar)
>y<-Sugar$ash
>x<-Sugar$wave.290
>z<-Sugar$wave.240
>index.y.25 <- y > 25
```

```

>index.atip <- index.y.25
>(1:268)[index.atip]
[1] 71 129
>x.sug <- x[!index.atip,]
>z.sug<- z[!index.atip,]
>y.sug <- y[!index.atip]
>train<-1:216

```

The following code demonstrates the implementation of the MFPLM using the functions `PVS.kernel.fit()` and `PVS.kNN.fit()`. We have chosen a semimetric based on derivatives, specified as `semimetric="deriv"` with `q=0` (default options). In each stage of the two-step procedures, we use half of the sample, setting $n_1 = n_2 = 108$ by defining `train.1=1:108` and `train.2=109:216`. Consequently, $n_1 > w_n$, but n_2 may be smaller than the cardinality of \mathcal{R} (denoted as $\#\mathcal{R}$). In such cases, it is advisable to specify `lambda.min.h`, `lambda.min.l`, and `factor.pn` to adjust the level of penalisation in each step of the PVS. Therefore, we set `lambda.min.l=0.05`, `lambda.min.h=0.08`, and `factor.pn=1`. This ensures that if $n_2 < \#\mathcal{R}$, then `lambda.min=0.08`; otherwise, `lambda.min=0.05`.

```

>fit5 <- PVS.kNN.fit(x=x.sug[train,],z=z.sug[train,], y=y.sug[train],train.1=1:108,
train.2=109:216, lambda.min.l=0.05,lambda.min.h=0.08, max.knn=10,nknot=20,
criterion="BIC")

```

```

>fit6 <- PVS.kernel.fit(x=x.sug[train,],z=z.sug[train,], y=y.sug[train], train.1=1:108,
train.2=109:216, lambda.min.l=0.05,lambda.min.h=0.08, num.h = 10, max.q.h=0.35,
nknot=20,criterion="BIC")

```

The objects `fit5` and `fit6` belong to an S3 class (see Table 8), which implements S3 methods. The functionalities of these methods were detailed throughout the case studies in Sections 2.3.2, 3.3.2, and 4.3.2. They include displaying a summary of the fitted models using `summary.PVS.kNN()` and `summary.PVS.kernel()`, respectively (alternatively, `print.PVS.kNN()` and `print.PVS.kernel()` can be used); obtaining graphical representations of the outputs through `plot.PVS.kNN()` and `plot.PVS.kernel()`; and making predictions for the fitted objects using `predict.PVS.kNN()` and `predict.PVS.kernel()`, respectively. These latter functions implement the three prediction possibilities outlined in Section 4.3.2. In addition, `predict.PVS.kNN()` implements `option=4`, which involves reselecting k for predicting the functional nonparametric component of the model, but this time in a local manner. This selection is performed using the LOOCV criterion in the functional nonparametric model, applied to the complete training sample (i.e., `train=c(train.1,train.2)`).

Table 10 shows the MSEP, setting `option=2`, and \hat{s}_n for each primary fitting function listed in Table 8 allowing for 2 curves in the model (i.e., the MFPLM and MFPLSIM fitting functions). The results were obtained using the respective BIC selectors for λ , w_n , and h/k in two different scenarios: (i) `lambda.min=0.05` (i.e., `lambda.min.h=lambda.min.l=0.05`) and (ii) `lambda.min=0.05` and `lambda.min=0.08`, with `factor.pn=1`. It should be noted that in the 1-step procedures (`FASSMR.kernel.fit()` and `FASSMR.kNN.fit()`), the same results will be obtained in both scenarios (i) and (ii) as long as $n > \text{factor.pn} * w_n$. For comparative purposes, the same values for common input arguments were used across all six functions. Additionally, h and k were selected using the same input options:

setting `max.knn=10` for k NN-based estimation functions and `max.q.h=0.35` for kernel-based ones. The remaining arguments were set to their default options.

It is noteworthy that both the MFPLM and MFPLSIM fitting functions improve their predictive ability by setting `lambda.min.h=0.08`. Additionally, under this setting, they tend to select an equal or lower number of impact points, leading to a simpler model. The functions fitting the MFPLSIM show a more significant improvement in MSEP and a greater reduction in the number of impact points selected. However, the best result in terms of MSEP is provided by the MFPLM fitted using `PVS.knn.fit()`.

Model	Function	lambda.min=0.05		lambda.min.l=0.05 lambda.min.h=0.08	
		MSEP	\hat{s}_n	MSEP	\hat{s}_n
MFPLM	<code>PVS.kernel.fit()</code>	2.00	10	1.92	9
	<code>PVS.knn.fit()</code>	1.20	7	1.19	7
MFPLSIM	<code>FASSMR.kernel.fit()</code>	4.70	6	4.70	6
	<code>FASSMR.knn.fit()</code>	3.60	8	3.60	8
	<code>IASSMR.kernel.fit()</code>	3.28	11	2.44	5
	<code>IASSMR.knn.fit()</code>	3.29	8	1.85	4

Table 10: MSEP obtained for each function using the respective BIC selectors for the tuning parameters (λ , w_n and h or k).

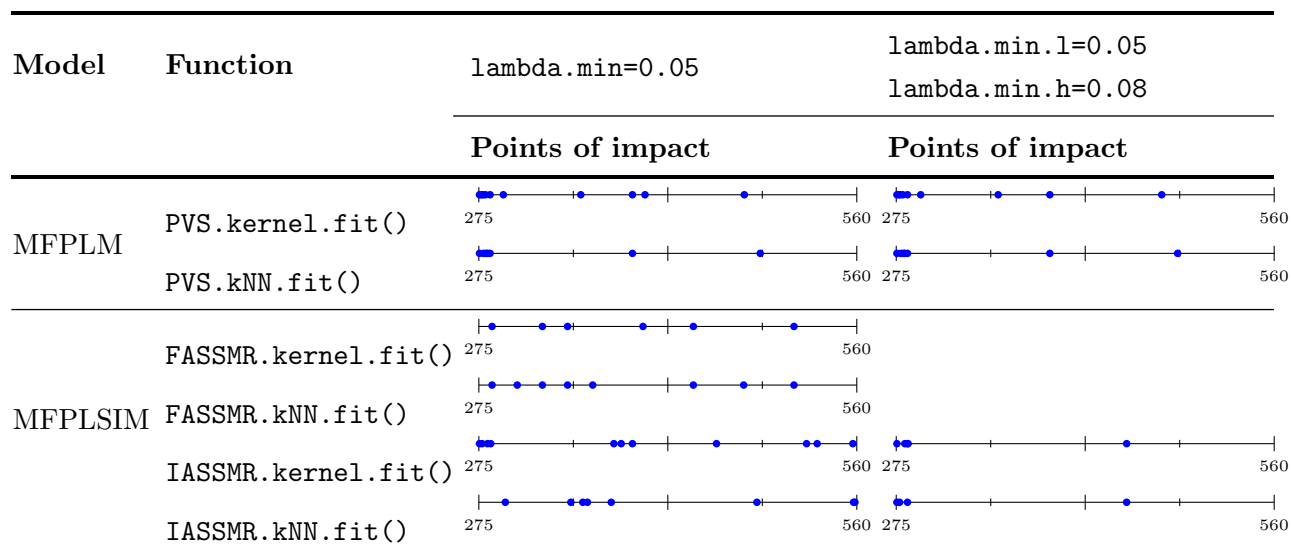


Table 11: Impact points obtained for each function using the respective BIC selectors for the tuning parameters (λ , w_n and h or k).

To gain a deeper understanding, Table 11 displays (as explained in Section 4.3.2) the impact points selected by the six main functions in scenarios (i) and (ii). In the case of 1-step functions, the selection

remains the same under both scenarios, as previously detailed. Comparing the results of each method in the two settings, it is noteworthy that the PVS functions obtain almost the same impact point selection: exactly the same using the `PVS.kNN.fit()` function, and with just one additional impact point using `PVS.kernel.fit()`. However, for the IASSMR functions, there is a significant change in the impact point selection, both in the number and position of the impact points. This fact explains the substantial change in MSE_P in the two scenarios.

Analysing the results in scenario (ii) for the two-step functions, we observe four distinct clusters of impact points. It appears that all algorithms consistently select a set of observations at the beginning of the first quartile of the timeline. Additionally, both IASSMR algorithms select an impact point in the middle of the third quartile, while the PVS algorithms choose it at the end of the third quartile. Furthermore, PVS procedures select another point at the end of the second quartile and `PVS.kNN.fit()` also selects an impact point at the beginning of the second quartile.

Combining the information from Tables 10 and 11, the best choice of points appears to be made by the function `PVS.kNN.fit()`. Furthermore, in this real data analysis, it seems that the second step plays a crucial role in the IASSMR algorithms, as the results provided in MSE_P and impact point selection by the IASSMR are substantially worse.

5 Discussion

This article introduces a new R package, `fsemipar` (see [Aneiros and Novo 2024](#)), tailored for SoF semi-parametric regression. The package implements various models with at least one functional predictor. The effects included for functional covariates are functional single-index, functional nonparametric, and pointwise linear. The link function of functional single-index components and the functional operator of the functional nonparametric ones are estimated using kernel smoothing techniques. This includes not only kernel-based estimation but also k NN-based estimation, allowing for both global and local smoothing. In the case of the pointwise linear effect of curves, the package includes algorithms to handle the high dependence between the discretized observations, allowing the selection of points of impact. This feature has proven to be highly beneficial from a predictive perspective in the real data applications included in the article.

The package `fsemipar` also allows the inclusion of scalar variables as predictors with a linear effect, enabling simultaneous estimation and variable selection using penalised least-squares procedures. Through the real data applications, the article demonstrates the capabilities of the package, providing a comprehensive review of its features. Despite the large number of optional arguments for each function, all functions require only the data as a mandatory argument, facilitating easy use.

Despite the wide range of possibilities it currently offers, the package will continue to be updated, striving to enhance its functionalities. This includes optimizing the computational cost of functions that estimate functional single-index components, exploring implementations in C++ using the `Rcpp` or `RcppArmadillo` packages. It also involves incorporating goodness-of-fit tests for functional semi-parametric regression (see, e.g., [Chan et al. 2023](#)), and increasing the flexibility of the included models. Enhancements may involve increasing the flexibility in the effect of scalar variables. For instance, this could include accounting for measurement errors (see, e.g., [Zhu et al. 2020](#)) and varying coefficients (see, e.g., [Wu et al. 2010](#)), or handling responses that are missed at random (see, e.g., [Ling et al.](#)

2019).

References

- Ait-Saïdi, A., Ferraty, F., Kassa, R., and Vieu, P. (2008). Cross-validated estimations in the single-functional index model. *Statistics*, 42(6):475–494.
- Amato, U., Antoniadis, A., and De Feis, I. (2006). Dimension reduction in functional regression with applications. *Computational Statistics & Data Analysis*, 50(9):2422–2446.
- Aneiros, G., Ferraty, F., and Vieu, P. (2015). Variable selection in partial linear regression with functional covariate. *Statistics*, 49(6):1322–1347.
- Aneiros, G. and Novo, S. (2024). *fsemipar: Estimation, Variable Selection and Prediction for Functional Semiparametric Models*. R package version 1.1.1.
- Aneiros, G., Novo, S., and Vieu, P. (2022). Variable selection in functional regression models: A review. *Journal of Multivariate Analysis*, 188:104871.
- Aneiros, G. and Vieu, P. (2014). Variable selection in infinite-dimensional problems. *Statistics & Probability Letters*, 94:12–20.
- Aneiros, G. and Vieu, P. (2015). Partial linear modelling with multi-functional covariates. *Computational Statistics*, 30(3):647–671.
- Aneiros-Pérez, G. and Vieu, P. (2006). Semi-functional partial linear regression. *Statistics & Probability Letters*, 76(11):1102–1110.
- Boente, G. and Vahnovan, A. (2017). Robust estimators in semi-functional partial linear regression models. *Journal of Multivariate Analysis*, 154:59–84.
- Breheny, P. and Huang, J. (2011). Coordinate descent algorithms for nonconvex penalized regression, with applications to biological feature selection. *The Annals of Applied Statistics*, 5(1):232 – 253.
- Breheny, P. and Huang, J. (2015). Group descent algorithms for nonconvex penalized linear and logistic regression models with grouped predictors. *Statistics and Computing*, 25:173–187.
- Brockhaus, S., Rügamer, D., and Greven, S. (2020). Boosting functional regression models with FDboost. *Journal of Statistical Software*, 94(10):1–50.
- Burba, F., Ferraty, F., and Vieu, P. (2009). k-Nearest Neighbour method in functional nonparametric regression. *Journal of Nonparametric Statistics*, 21(4):453–469.
- Cardot, H., Ferraty, F., and Sarda, P. (1999). Functional linear model. *Statistics and Probability Letters*, 45(1):11–22.
- Chan, L., Delsol, L., and Goia, A. (2023). A link function specification test in the single functional index model. *Advances in Data Analysis and Classification*.

- Collomb, G. (1979). Estimation de la régression par la méthode des k points les plus proches: propriétés de convergence ponctuelle, (French). *Comptes Rendus de l'Académie des Sciences*, pages 245–247.
- Dai, W. and Genton, M. G. (2018). Multivariate functional data visualization and outlier detection. *Journal of Computational and Graphical Statistics*, 27(4):923–934.
- De Boor, C. (1978). *A practical guide to splines*, volume 27. springer-verlag New York.
- Devroye, L., Györfi, L., Krzyżak, A., and Lugosi, G. (1994). On the Strong Universal Consistency of Nearest Neighbor Regression Function Estimates. *The Annals of Statistics*, 22(3):1371 – 1385.
- Fan, J. (1997). Comments on “Wavelets in Statistics: A review” by A. Antoniadis. *Journal of the Italian Statistical Society*, 6:131.
- Fan, J. and Li, R. (2001). Variable selection via nonconcave penalized likelihood and its oracle properties. *Journal of the American Statistical Association*, 96(456):1348–1360.
- Febrero-Bande, M., Galeano, P., and González-Manteiga, W. (2017). Functional principal component regression and functional partial least-squares regression: An overview and a comparative study. *International Statistical Review*, 85(1):61–83.
- Febrero-Bande, M. and González-Manteiga, W. (2013). Generalized additive models for functional data. *Test*, 22:278–292.
- Febrero-Bande, M. and Oviedo de la Fuente, M. (2012). Statistical computing in functional data analysis: The R package *fda.usc*. *Journal of Statistical Software*, 51(4):1–28.
- Ferraty, F., Goia, A., Salinelli, E., and Vieu, P. (2013). Functional projection pursuit regression. *Test*, 22:293–320.
- Ferraty, F., Peuch, A., and Vieu, P. (2003). Modèle à indice fonctionnel simple. *Comptes Rendus Mathématique de l'Académie des Sciences Paris*, 336(12):1025–1028.
- Ferraty, F. and Vieu, P. (2006). *Nonparametric Functional Data Analysis, Theory and Practice*. Springer Series in Statistics. Springer-Verlag, New York.
- Galeano, P., Joseph, E., and Lillo, R. E. (2015). The mahalanobis distance for functional data with applications to classification. *Technometrics*, 57(2):281–291.
- Goldsmith, J., Scheipl, F., Huang, L., Wrobel, J., Di, C., Gellar, J., Harezlak, J., McLean, M. W., Swihart, B., Xiao, L., Crainiceanu, C., and Reiss, P. T. (2023). *refund: Regression with Functional Data*. R package version 0.1-32.
- Greven, S. and Scheipl, F. (2017). A general framework for functional regression modelling. *Statistical Modelling*, 17(1-2):1–35.
- Kara-Zaitri, L., Laksaci, A., Rachdi, M., and Vieu, P. (2017a). Data-driven kNN estimation in nonparametric functional data analysis. *Journal of Multivariate Analysis*, 153:176–188.

- Kara-Zaitri, L., Laksaci, A., Rachdi, M., and Vieu, P. (2017b). Uniform in bandwidth consistency for various kernel estimators involving functional data. *Journal of Nonparametric Statistics*, 29(1):85–107.
- Kneip, A., Poß, D., and Sarda, P. (2016). Functional linear regression with points of impact. *The Annals of Statistics*, 44(1):1 – 30.
- Li, Y., Huang, C., and Härdle, W. K. (2019). Spatial functional principal component analysis with applications to brain image data. *Journal of Multivariate Analysis*, 170:263–274. Special Issue on Functional Data Analysis and Related Topics.
- Ling, N., Kan, R., Vieu, P., and Meng, S. (2019). Semi-functional partially linear regression model with responses missing at random. *Metrika*, 82(1):39–70.
- Ling, N. and Vieu, P. (2018). Nonparametric modelling for functional data: selected survey and tracks for future. *Statistics*, 52(4):934–949.
- Ling, N. and Vieu, P. (2021). On semiparametric regression in functional data analysis. *WIREs Computational Statistics*, 13(6):e1538.
- McKeague, I. W. and Sen, B. (2010). Fractals with point impact in functional linear regression. *The Annals of Statistics*, 38(4):2559 – 2586.
- McLean, M. W., Hooker, G., Staicu, A.-M., Scheipl, F., and Ruppert, D. (2014). Functional generalized additive models. *Journal of Computational and Graphical Statistics*, 23(1):249–269. PMID: 24729671.
- Nadaraya, E. A. (1964). On estimating regression. *Theory of Probability and Application*, 9:141–142.
- Novo, S., Aneiros, G., and Vieu, P. (2019). Automatic and location-adaptive estimation in functional single-index regression. *Journal of Nonparametric Statistics*, 31(2):364–392.
- Novo, S., Aneiros, G., and Vieu, P. (2021a). Sparse semiparametric regression when predictors are mixture of functional and high-dimensional variables. *TEST*, 30:481–504.
- Novo, S., Vieu, P., and Aneiros, G. (2021b). Fast and efficient algorithms for sparse semiparametric bi-functional regression. *Australian and New Zealand Journal of Statistics*, 63:606–638.
- Preda, C. and Saporta, G. (2005). PLS regression on a stochastic process. *Computational Statistics & Data Analysis*, 48(1):149–158.
- R Core Team (2022). *R: A Language and Environment for Statistical Computing*. R Foundation for Statistical Computing, Vienna, Austria.
- Ramsay, J. O., Graves, S., and Hooker, G. (2022). *fda: Functional Data Analysis*. R package version 6.0.5.
- Ramsay, J. O. and Silverman, B. (2005). *Functional Data Analysis*. Springer Series in Statistics. Springer-Verlag, New York, 2nd edition.

- Reiss, P. T., Goldsmith, J., Shang, H. L., and Ogden, R. T. (2017). Methods for scalar-on-function regression. *International Statistical Review*, 85(2):228–249.
- Rice, G., Wirjanto, T., and Zhao, Y. (2020). Tests for conditional heteroscedasticity of functional data. *Journal of Time Series Analysis*, 41(6):733–758.
- Scheipl, F., Arnone, E., Hooker, G., Tucker, J. D., and Wrobel, J. (2022). *CRAN Task View: Functional Data Analysis*. Version 2022-03-21.
- Tibshirani, R. (1996). Regression shrinkage and selection via the LASSO. *Journal of the Royal Statistical Society: Series B*, 58:267–288.
- Wang, G., Feng, X.-N., and Chen, M. (2016). Functional partial linear single-index model. *Scandinavian Journal of Statistics*, 43(1):261–274.
- Wang, L., Chen, G., and Li, H. (2007). Group SCAD regression analysis for microarray time course gene expression data. *Bioinformatics*, 23(12):1486–1494.
- Watson, G. (1964). Smooth regression analysis. *Sankhyā: The Indian Journal of Statistics Series A*, 26:359–372.
- Wu, Y., Fan, J., and Müller, H.-G. (2010). Varying-coefficient functional linear regression. *Bernoulli*, 16(3):730 – 758.
- Yuan, M. and Lin, Y. (2005). Model Selection and Estimation in Regression with Grouped Variables. *Journal of the Royal Statistical Society Series B: Statistical Methodology*, 68(1):49–67.
- Zhu, H., Zhang, R., and Zhu, G. (2020). Estimation and inference in semi-functional partially linear measurement error models. *Journal of Systems Science and Complexity*, 33:1179–1199.